Zoosyst. Evol. 101 (2) 2025, 813–853 | DOI 10.3897/zse.101.137663

PENSOFT. MUSEUM FÜR NATURKUNDE BERLIN

Across trench and ridge: description of five new species of the *Haploniscus belyaevi* Birstein, 1963 species complex (Isopoda, Haploniscidae) from the Kuril-Kamchatka Trench region

Henry Knauber[1,2], Tilman Schell[3], Angelika Brandt[1,2], Torben Riehl[1,2]

1 *Senckenberg Research Institute and Natural History Museum, Department of Marine Zoology, Section Crustacea, Senckenberganlage 25, 60325 Frankfurt, Germany*

2 *Johann Wolfgang Goethe University Frankfurt, Department of Biological Sciences, Institute of Ecology, Evolution and Diversity, Max-von-Laue-Str. 13, 60438 Frankfurt, Germany*

3 *LOEWE-Centre for Translational Biodiversity Genomics (LOEWE-TBG), 60438 Frankfurt, Germany*

https://zoobank.org/1764B434-B419-4430-B297-6D6380572DFB

Corresponding author: Henry Knauber (henry.knauber@senckenberg.de)

Academic editor: Luiz F. Andrade ♦ **Received** 23 September 2024 ♦ **Accepted** 11 March 2025 ♦ **Published** 22 April 2025

Abstract

Integrative taxonomy provides a valuable approach to discover and unravel even morphologically almost indiscernible species, such as those forming “cryptic” species complexes. The six members of the recently discovered *Haploniscus belyaevi* species complex (short: *belyaevi*-complex) from the abysso-hadal Kuril-Kamchatka Trench (KKT) region in the Northwest Pacific Ocean are taxonomically described herein. The eponymous *Haploniscus belyaevi* is redescribed alongside new descriptions of the five closely related species *Haploniscus apaticus* **sp. nov.**, *H. erebus* **sp. nov.**, *H. hades* **sp. nov.**, *H. kerberos* **sp. nov.**, and *H. nyx* **sp. nov.** The morphological differences between these species are most eminent in the rostral and pleotelson morphology of the adult males. Alongside light-microscopical drawings, CLSM scans, and 16S and COI barcodes, these species descriptions are complemented by the first genomic data of deep-sea haploniscid isopods. Geometric morphometrics was applied to quantify interspecific and intraspecific morphological differences of the pleotelson considering the pronounced sexual dimorphism. The distributional range of the *belyaevi*-complex covers a large geographical area, ranging across the greater KKT region and extending beyond large-scale geomorphological barriers such as the KKT and the Kuril Island Ridge, turning these into promising species to study differentiation processes in the deep sea.

Key Words

Asellota, biological systematics, CLSM, genomics, Janiroidea, mitogenome, Peracarida, Sea of Okhotsk

Introduction

Attempts to catalogue the biodiversity of the largest yet least explored biome of the world, the deep sea, have been ongoing for decades and remain far from complete. Estimations suggest up to 91% of marine species are yet to be discovered (Mora et al. 2011; but see also Appeltans et al. 2012). Species complexes – closely related taxa that often exhibit minuscule morphological differences (e.g., “cryptic” species) – are numerous amongst many phyla and taxonomic groups, e.g., Bivalvia (Goffredi et al. 2003), Crinoidea (McLaughlin et al. 2023), Decapoda (Silva et al. 2021), or Isopoda (Schnurr et al. 2018). Yet, the discovery of marine biodiversity is especially complicated by a high proportion of species that are difficult to discriminate, including “cryptic” species as well as those with relatively strong phenotypic plasticity, di- and polymorphisms, and significant morphological changes during their ontogenetic development (e.g., Knowlton 1993; Vrijenhoek 2009; Riehl et al. 2012). However, an

Copyright *Knauber, H. et al.* This is an open access article distributed under the terms of the Creative Commons Attribution License (CC BY 4.0), which permits unrestricted use, distribution, and reproduction in any medium, provided the original author and source are credited.

integrative taxonomic framework has proven useful in discriminating "cryptic" species and revealing new species even in such difficult cases.

For deep-sea biodiversity studies, where sample sizes are commonly small in light of low abundances and patchy distributions, species are often represented by only a few individuals (Rex and Etter 2010). Yet, as explained above, without knowing the full phenotypic variability, cataloging species richness can be a challenge. Johannsen et al. (2020) faced such a situation, leading Knauber et al. (2022) to use an integrative taxonomic approach to study patterns of phenotypic variation in a species of haploniscid isopods from the Kuril-Kamchatka Trench region in the Northwest Pacific Ocean. Initially believed to represent a single species, *Haploniscus belyaevi* Birstein, 1963, the collected material turned out to comprise at least six distinct species, five of which were new to science (see also Johannsen et al. 2020).

Haploniscidae Hansen, 1916, is a relatively common and cosmopolitan family of asellote isopods inhabiting soft sediments in the deep sea. Haploniscids occur from shallow to hadal depths. Currently, over 120 species of haploniscid isopods are known to science (Boyko et al. 2023), and a major taxonomic revision of the family has been called for, as relationships are largely unresolved and the largest genus, *Haploniscus* (Richardson, 1908), serves as a repository for species that lack clear apomorphies or affinities to the remaining genera. The discovery of the *belyaevi*-complex is by no means the first record of a species complex within this family: Brökeland and Raupach (2008) and Brökeland (2010a) described two other species complexes within the Haploniscidae, emphasizing the need for a major taxonomic revision of the systematically unstructured family.

In this study the newly discovered species of the *belyaevi*-complex are formally described, and *H. belyaevi* is redescribed with new neotypes assigned. Besides classical morphological methods and DNA barcoding, geometric morphometric analyses and genome sequencing were utilized, two approaches novel for haploniscid species descriptions.

Methods

Study area and sampling

The study region covers the central part of the Kuril-Kamchatka Trench (KKT) in the Northwest Pacific Ocean (NWP) and adjacent abyssal seabed, also including the marginal Sea of Okhotsk (SO). Located in a highly productive area, the KKT extends from the Japanese island Hokkaido in the southwest alongside the Kuril Island Ridge (KIR) to the coasts of the Russian peninsula Kamchatka in the northeast. With depths of up to 9,600 m (Dreutter et al. 2020), the KKT represents one of the deepest hadal regions in the Pacific Ocean and forms a link between the Japan and Aleutian Trenches. Neighboring the trench to the southeast are vast abyssal plains of the open NWP, while the marginal SO and its Kuril Basin (3,374 m max. depth) in the northwest are separated from the KKT and the NWP by the Kuril Islands. Several bathyal straits, such as the Bussol Strait (2,350 m sill depth) or Krusenstern Strait (1,920 m sill depth), allow for the exchange of water and potentially deep-sea fauna between the KKT and the SO (Tyler 2002; Malyutina et al. 2018). Between 2012 and 2016, the benthos of both the KKT and the SO has been investigated during three successive deep-sea expeditions, namely the KuramBio (KB), KuramBio II (KBII), and SokhoBio (SKB) campaigns (Brandt and Malyutina 2013; Malyutina et al. 2015; Brandt 2016). These expeditions aimed to complement the inventory of the benthic biodiversity of the greater KKT region established in the mid-twentieth century by Russian investigators (Monin 1983; Golovan et al. 2019; Brandt et al. 2020), understand species ranges and turnover and their driving forces, and investigate potential barrier effects of the KKT and the KIR on deep-sea fauna. The distribution map was created using QGIS 3.28 with GRASS 7.8.7 (GRASS Development Team 2020; QGIS.org 2020).

All haploniscid samples examined for this study were collected during the SokhoBio (Sea of Okhotsk Biodiversity Studies; Malyutina et al. 2018) campaign on board the RV *Akademik M.A. Lavrentyev* in 2015 and the KuramBio II (Kuril Kamchatka Biodiversity Studies II, Brandt 2016) campaign on board the RV *Sonne* in the KKT and SO regions. The samples referred to in this study were collected using a box corer (BC; Hessler and Jumars 1974), an Agassiz trawl (AGT; Agassiz 1880), and an epibenthic sledge with 300 µm-meshed cod ends (Brenke 2005; EBS; Brandt et al. 2013). The collected sediment was sieved on board using 300 µm-meshed metal sieves and filtered with −20 °C precooled, filtered seawater to remove fine sediment fractions. Thereafter, samples were bulk fixed in chilled 96% ethanol and kept chilled at all times to prevent DNA degradation, following Riehl et al. (2014).

Taxonomy

Following recent publications on the sexual dimorphic haploniscid isopods, the species descriptions focus on the adult males as holotypes (see Fig. 1), while adult females are used and described as paratypes (Brökeland and Raupach 2008; Brökeland 2010a; Brökeland and Svavarsson 2017). The designation and nomenclature of ontogenetic stages follow Knauber et al. (2022).

The material was examined using a stereomicroscope, the Leica M60, to assign type specimens for subsequent taxonomic analysis. To designate a type locality for each novel species, special emphasis was laid on selecting holo- and paratype specimens from the same or neighboring sampling areas, which also include the specimens used for genome analyses (see below). Voucher photos were taken using a LEICA M165C equipped with a LEICA DMC5400 camera utilizing the LAS-X software. Taxonomic drawings of each specimen were prepared using a Leica DM 2500 LED microscope equipped with a *camera lucida*. While pereopods, pleopods, and mouthparts were dissected, the

antennae were illustrated *in situ* to prevent potential damage to the head of the type specimens. To prepare the specimens for drawing and confocal laser scanning microscopy (CLSM), they were transferred from 70–96% EtOH to a 1:1 solution of 70% EtOH and glycerin and set aside for two days, letting the ethanol evaporate slowly to avoid potential shrinking of the specimens. Subsequently, they were transferred to 80% glycerin, and temporary slides were prepared following the method of Wilson (2008). The resulting pencil drawings were digitalized using the Adobe Illustrator 27.2 software, following Coleman (2003).

For the CLSM, the samples were stained using Congo Red dissolved in 70% denatured EtOH while remaining in glycerine following Michels and Büntzow (2010). After placing the samples on temporary slides, scans were conducted using a Leica DM2500 with a Leica TCS SPE II and the LEICA LAS X 3.5.5.19976 software at a resolution of 2480 × 2480 pixels. Post-production of the resulting CLSM scans was carried out in Adobe Photoshop 24.1.1 and Adobe Illustrator 27.2.

Based on the voucher images, CLSM scans, and digitalized drawings, all specimens were measured using the measuring tool in Adobe Acrobat Pro, building upon the standards of Hessler (1970). The body length was measured from a lateral view under consideration of potential body curvature from the frontal margin of the head to the posterior medial margin of the pleotelson, thus excluding rostrum and pleotelsonic processes from the total body length. All other measurements regarding body segment lengths were taken from the dorsal habitus drawings along the specimens' midline. Generally, the total length of appendages like antennae or pereopods was measured along the midline of each segment.

For the species description, a taxonomic character database for the Haploniscidae developed in the DELTA system (Dallwitz 1980; Dallwitz et al. 1999) was used (SOSA et al. 2024). The preparation of the taxonomic characters and their character states within the DELTA database included literature research on haploniscid taxonomy papers with special emphasis on characters used for species delimitation. Morphological terminology was based on Brökeland and Svavarsson (2017) with modifications. Setae were named after Riehl and Brandt (2010).

Molecular diagnoses based on barcodes of the mitochondrial large ribosomal RNA subunit (16S) and the cytochrome-c-oxidase subunit I (COI) were prepared using the online tool DeSigNate (Hütter et al. 2020), only focusing on alignment positions with a discriminative power of 1.0.

The material of the herein described species is deposited at the Senckenberg Museum Frankfurt, Germany (SMF), the Zoological Museum Hamburg, Germany (ZMH), and the Museum of Institute of Marine Biology, Vladivostok, Russia (MIMB).

Haploniscid species description standards

Historically, janiroidean species descriptions became more and more lengthy over time, as taxonomists attempted to describe new species in a complete and detailed fashion, often incorporating characters without species delimitating potential. Leaning on a recent description template (SOSA et al. 2024), this study prioritized the illustration of characters over their extensive description in the form of text. To achieve this, the focus was on apomorphic characters useful for species delimitation, whilst most plesiomorphic characters and such of descriptive nature were only omitted from the descriptions. Characters omitted from the text comprise the mostly plesiomorphic mouthparts, pleopods III–V, and most setation patterns on antennae, pereopods, and pereonites. Nevertheless, all these structures have been depicted in the provided illustrations, considering the possibility that future reassessments may still discover their value in species delimitation. Likewise, recurring features were only presented once in text form, such as in the case of the pereopods. The description of the female paratypes with a more uniform morphology is restricted to characters in which these specimens differ from their male counterparts. Pereopod I was drawn and described due to more pronounced setation patterns in its distal segments in comparison to the remaining pereopods, of which only pereopods II and VI were depicted, as pereopods II through VII differ only in length and length-dependent ratios. With pereopod II being the shortest and pereopod VI the longest of these otherwise uniform legs, we solely depict their extremes.

The species descriptions also feature molecular diagnoses based on 16S and COI barcodes to facilitate differentiation on molecular data.

Geometric morphometrics

Most haploniscid species can be told apart based on the morphology of the antenna, the rostrum, and the pleotelson, of which the latter is the easiest to study in a standardized way. Therefore, the pleotelson shape was studied from a ventral view using geometric morphometrics (GM) and a combination of CLSM scans and photographs. Due to a low specimen count for several of the herein discussed species, these analyses were restricted to adult specimens of *H. belyaevi*, *H. kerberos* sp. nov., and *H. hades* sp. nov. The CLSM scans and photographs were then processed and statistically analyzed using the tps software suite (Rohlf 2015) and MorphoJ 1.07a (Klingenberg 2011) following the approach described in Casaubon and Riehl (2024). Subsequently, Adobe Illustrator 27.2 was used to adjust the resulting plot.

Genome sequencing

Genome sequencing was conducted for five of the six members of the *belyaevi* complex, alongside another haploniscid species, *H. hydroniscoides* Birstein, 1963, for means of comparison. Given the low available specimen count for *H. nyx* sp. nov., no specimen of this species was chosen for genome sequencing. DNA isolation was conducted at Loewe TBG, Frankfurt, Germany, while sequencing was carried out by Novogene in Cambridge, UK.

A thorough description of the methods used for the nuclear and mitochondrial genome assembly can be found in Suppl. material 1. In brief, nuclear genome assemblies were conducted using Spades 3.15.0 (Prjibelski et al. 2020) and Platanus 1.2.4 (Kajitani et al. 2014) after quality filtering with Trimmomatic 0.39 (Bolger et al. 2014). From the resulting contigs, contamination and sequences with mitochondrial origin were filtered out, and final assemblies were assessed regarding quality with Quast (Gurevich et al. 2013) and BUSCO 5.5.0 (Manni et al. 2021). Raw Illumina reads were used alongside available COI sequences from the respective specimens (BOLD acc. no. NWPHA090-20, NWPHA107-20, NWPHA138-20, NWPHA223-20, NWPHA267-20, NWPHA268-20) as a seed for input in NOVOplasty 4.2 (Dierckxsens et al. 2017) to assemble the mitochondrial genome of each sample. The annotation of the mitochondrial genomes was conducted by manually combining and curating annotations from GeSeq (Tillich et al. 2017) and MITOS2 (Donath et al. 2019) in Geneious Prime 2020.2.3 (https://www.geneious.com) per species. Mitogenome data of two preliminary species of the munnopsid genus *Notopais* were extracted from GenBank (Benson et al. 2012; acc. no. OL661185 and OL661186) as an outgroup for subsequent analyses on interspecific divergence. Thereafter, matrices of pairwise distances were calculated for the resulting mitogenome dataset using MEGA11 v11.0.11 (Tamura et al. 2021).

Abbreviations

A—Antenna; **Ceph**—Cephalothorax; **Md**—Mandible; **Mxp**—Maxilliped; **P**—Pereopod; **Plp**—Pleopod; **Plt**—Pleotelson; **Prn**—Pereonite.

Results

Taxonomy

Family Haploniscidae Hansen, 1916
Genus *Haploniscus* Richardson, 1908

***Haploniscus belyaevi* species complex**

Composition. *Haploniscus belyaevi* Birstein, 1963, *H. apaticus* sp. nov., *H. erebus* sp. nov., *H. hades* sp. nov., *H. kerberos* sp. nov., *H. nyx* sp. nov.

Diagnosis. Haploniscidae with a dorsoventrally elliptical body, non-conglobating; tergite surfaces tuberculate, ornamentation evenly distributed, convex cross-section of tergites broken by slight, uneven elevations at the muscle attachment points of pereopods, elevated areas without ornamentation (see Fig. 1). Ceph trapezoidal, tuberculate; anterolateral angles rounded, not projecting; acute rostrum, basally with ventral bulge. At least Prn 1 posterior tergite margin through Prn 5 anterior tergite margin delicately serrated, setose; at least Prn 2 anterolateral angle through Prn 4 posterolateral angle with minute, acute projections; Prn 1–7 posterolateral angles asetose; Prn 7 of similar shape as previous Prns; Prn 7 and Plt tergites medially conjoint, segment borders not expressed. Plt dorsally with a pair of tubercles; posterolateral processes tapering to acute tips. AII article 3 slightly longer than wide, dorsal projection oriented anteriorly; article 5 with elongated and acute distolateral projection. Mandible palp distinctly longer than mandible, palp article 2 curved. All P carpi, propodi, and dactyli dorsal margins fringed by comb-like scale rows. Male Plp I proximal part trapezoid; lateral lobes indistinct, fused with medial lobes. Male Plp II protopod distal margin with continuous row of elongated simple setae, lateral margin with 1–3 short simple setae, endopod stylet very long, distinctly longer than protopod. Female operculum anteriorly with median bulge, otherwise circular, smooth. Uropods cylindrical, projecting caudally beyond posterior Plt apex, recessed in sternal fold laterally to anal valve.

Remarks. Species of the *belyaevi*-complex can be easily recognized amongst congeners by the two antennal spines located on the third and fifth peduncular articles of the second antennae. While antennal spines on the third article are fairly common amongst haploniscids, the presence of a second, large, and distal spine on the antennal fifth article is a unique feature of the *belyaevi*-complex. The rostral process of the *belyaevi*-complex, despite minor interspecific differences, could only be confused with the rostrum of *H. profundicolus* (Birstein 1971) and is otherwise conspicuously different from other haploniscids from the Northwest Pacific Ocean. Outside of the NWP, similar rostrum shapes also featuring a ventral bulge can be found in *H. hamatus* Lincoln, 1985, and *H. ampliatus* Lincoln, 1985. As common for the Haploniscidae, also the species of the *belyaevi*-complex show a pronounced sexual dimorphism. The adult males are highly distinct (see Fig. 1), while the adult female counterparts look much more alike, especially in terms of their overall body and pleotelson shapes. As the species-specific characters of rostrum and pleotelson only fully emerge in the adult male stages, assigning manca and female stages remains difficult when only morphological characters are considered. A noteworthy observation regarding ontogenetic changes within this species complex is that the antennal spines on the fifth article are minute in ovigerous females, much smaller than in preceding stages, and to a degree that they are almost unnoticeable. A visualization of the molecular variation within the complex is provided in Table 1 (16S) and Table 2 (COI). The mitochondrial genome contains the expected 13 protein-coding genes and two rRNAs in a conserved order (see 4.3 Genomics) for all member species of the complex. Detailed station data on sampling locations of the *belyaevi*-complex and its member species are provided in Table 3.

Table 1. Overview of molecular variation in the 16S gene within members of the *belyaevi*-complex. Numbers in brackets following a species name refer to the specimen count used for the molecular diagnosis analysis. Bold letters with a grey background indicate apomorphic nucleotides at the given position. Letters in brackets indicate heterogeneous base calls at that position. n lists the number of apomorphic nucleotides for each species in the respective gene sequence.

Taxon	25	56	64	66	71	150	155	156	173	204	206	219	228	243	249	312	342	350	355	358	n
H. apaticus sp. nov. (8)	A	A	A	G	T	A	G	A	A	T	A	G	T	T	T	T	T	G	A	T	0
H. erebus sp. nov. (14)	A	**G**	**G**	**T**	**G**	**-**	**A**	**T**	A	**A**	**G**	G	A	**C**	T	T	**C**	**A**	**G**	**C**	14
H. belyaevi (31)	A	A	A	G	T	A	G	A	A	T	A	G	(T)	T	**C**	T	T	G	A	T	1
H. hades sp. nov. (27)	T	A	C	A	T	G	G	A	A	T	A	**A**	A	T	T	T	T	G	A	T	1
H. kerberos sp. nov. (22)	T	A	C	A	T	G	G	A	**G**	T	A	G	**G**	T	T	T	T	G	A	T	2
H. nyx sp. nov. (3)	**G**	A	A	A	T	A	G	A	A	T	A	G	T	T	T	**C**	T	G	A	T	2

Table 2. Overview of molecular variation in the COI gene within members of the *belyaevi*-complex. Numbers in brackets following a species name refer to the specimen count used for the molecular diagnosis analysis. Bold letters with a grey background indicate apomorphic nucleotides at the given position. Letters with a red background indicate incomplete base call information due to shorter sequence reads. Letters in brackets indicate heterogeneous base calls at that position. n lists the number of apomorphic nucleotides for each species in the respective gene sequence.

Taxon	61	69	91	103	124	148	151	154	193	199	206	211	217	220	232	256	268	284	286	298
H. apaticus sp. nov. (3)	A	**T**	T	A	T	A	C	C	T	A	C	G	G	**A**	A	A	G	C	T	G
H. erebus sp. nov. (8)	A	C	T	A	T	A	**T**	**T**	T	A	C	G	G	C	A	A	**T**	**T**	**A**	A
H. belyaevi (6)	A	C	T	A	T	A	C	C	T	**G**	C	G	G	C	A	A	G	C	T	G
H. hades sp. nov. (27)	A	C	T	**G**	T	A	C	C	T	A	C	**A**	**T**	C	**C**	**G**	(G)	C	T	G
H. kerberos sp. nov. (21)	**T**	C	**C**	A	T	A	C	C	T	A	C	G	G	C	A	A	G	C	T	**C**
H. nyx sp. nov. (3)	A	C	T	A	**C**	**G**	C	C	**C**	A	**T**	G	G	C	A	A	G	C	T	A

Taxon	301	304	313	328	334	346	349	352	364	370	376	385	388	409	412	418	430	436	442	451
H. apaticus sp. nov. (3)	G	T	A	C	T	T	G	C	**A**	G	C	T	A	T	**G**	C	A	C	T	A
H. erebus sp. nov. (8)	**C**	T	**G**	C	T	T	G	**T**	G	G	**G**	**C**	**C**	A	T	**T**	A	**A**	T	**T**
H. belyaevi (6)	G	T	A	C	**C**	T	G	C	G	(G)	**T**	T	A	**C**	**A**	C	A	C	T	A
H. hades sp. nov. (27)	A	A	A	**T**	T	T	**A**	C	**C**	**C**	C	T	T	A	T	C	A	T	**C**	A
H. kerberos sp. nov. (21)	A	A	A	C	T	**G**	G	C	T	G	C	T	T	A	(C)	C	**G**	T	T	A
H. nyx sp. nov. (3)	A	**C**	A	C	**G**	**C**	G	C	T	G	C	T	A	T	C	C	A	T	T	A

Taxon	469	472	475	481	496	499	502	508	520	553	556	562	565	571	592	607	625	628	649	n
H. apaticus sp. nov. (3)	**G**	C	**A**	A	G	T	A	G	T	T	**C**	A	A	T	A	T	A	G	A	7
H. erebus sp. nov. (8)	C	**G**	**G**	A	(G)	T	**G**	T	T	T	T	**G**	**G**	T	A	T	A	G	A	19
H. belyaevi (6)	T	(T)	T	A	G	T	A	T	T	T	T	A	A	T	**G**	T	A	G	A	6
H. hades sp. nov. (27)	**A**	(A)	(T)	A	G	**C**	A	(A)	T	A	T	(T)	A	**C**	A	A	(G)	A	A	13
H. kerberos sp. nov. (21)	C	A	(T)	A	G	T	A	G	T	A	T	C	A	T	A	**G**	**T**	G	**G**	8
H. nyx sp. nov. (3)	T	C	T	**G**	**T**	T	A	**C**	**C**	**G**	**G**	A	A	T	A	T	G	**C**	A	14

Haploniscus belyaevi Birstein, 1963

Figs 1–5, 26

Neotype. SKB Hap46, adult male (stage VI), 3.4 mm, MIMB 50300.

Paraneotypes. SKB Hap04, adult female (stage IV; genome), SMF 56521; SKB Hap24, adult female (stage IV), 3.2 mm, MIMB 50294; SKB Hap06, adult male (stage VI), 3.6 mm, SMF 56523.

Type material. As pointed out by Knauber et al. (2022), the original male syntype of *H. belyaevi* as depicted in the original species description was lost. Instead, the species' type material is lumped together with additional material of *Haploniscus menziesi* Birstein, 1963. Most specimens are in poor condition, lacking either the distal AII with the characteristic spine on the fifth peduncular article or the pleotelson, rendering identification beyond genus level difficult. Three specimens can be identified as members of the *belyaevi*-complex, yet, as all of them are (ovigerous) female stages, allocation to one of the herein described member species of the *belyaevi*-complex remains uncertain. The type material is missing associated information about the sampling locality, and as the original description by Birstein does not define a type locality, *H. belyaevi* does not possess a definite type locality.

Based on I) the lack of a definite type locality, II) the presence of multiple haploniscid species in the type material of *H. belyaevi*, III) the absence of the original male syntype, and IV) uncertainty about where the material at hand stems from and whether it represents the type material, *H. belyaevi* is considered a *nomen dubium*. In an attempt to resolve the taxonomic identity of *H. belyaevi*, the species is therefore defined by the illustrations depicted in the original description by Birstein (1963),

Table 3. SokhoBio (LV71) and KuramBio II (SO250) stations, where members of the *Haploniscus belyaevi*-complex were sampled. EBS = Epibenthic Sledge; AGT = Agassiz Trawl.

Station	Depth [m]	Gear	Date	Latitude, Longitude
LV71 01-08	3307	EBS	2015-07-10	46°08.8'N, 145°59.2'E
LV71 02-07	3352	EBS	2015-07-13	46°40.9'N, 147°28.5'E
LV71 04-09	3365	EBS	2015-07-17	47°13.6'N, 149°39.2'E
LV71 04-10	3366	EBS	2015-07-17	47°12.2'N, 149°36.7'E
LV71 07-03	3296	EBS	2015-07-22	46°54.6'N, 151°05.3'E
LV71 07-04	3287	EBS	2015-07-22	46°59.4'N, 151°05.4'E
LV71 09-06	3502	EBS	2015-07-26	46°16.1'N, 152°00.0'E
LV71 09-07	3374	EBS	2015-07-26	46°16.2'N, 152°03.1'E
LV71 10-06	4469	EBS	2015-07-28	46°07.7'N, 152°09.7'E
LV71 10-07	4469	EBS	2015-07-29	46°07.8'N, 152°10.3'E
LV71 11-06	3206	EBS	2015-08-01	45°35.3'N, 146°24.7'E
SO250 008	5136	EBS	2016-08-19	43°49.55'N, 151°46.25'E
SO250 010	5120	EBS	2016-08-20	43°49.43'N, 151°46.96'E
SO250 020	8191	AGT	2016-08-23	45°51.32'N, 153°50.08'E
SO250 028	6051	EBS	2016-08-25	45°54.43'N, 152°47.02'E
SO250 030	6181	EBS	2016-08-27	45°56.38'N, 152°56.70'E
SO250 040	7081	EBS	2016-08-29	45°38.00'N, 152°55.95'E
SO250 042	7123	EBS	2016-08-30	45°39.62'N, 152°56.39'E
SO250 065	5755	EBS	2016-09-09	45°09.85'N, 153°43.34'E
SO250 085	5265	EBS	2016-09-15	45°02.26'N, 151°02.14'E
SO250 086	5493	AGT	2016-09-15	45°00.43'N, 151°06.01'E
SO250 087	5492	EBS	2016-09-16	45°00.76'N, 151°05.53'E
SO250 097	6575	EBS	2016-09-18	44°05.68'N, 151°24.88'E
SO250 098	6446	AGT	2016-09-19	44°05.53'N, 151°24.25'E

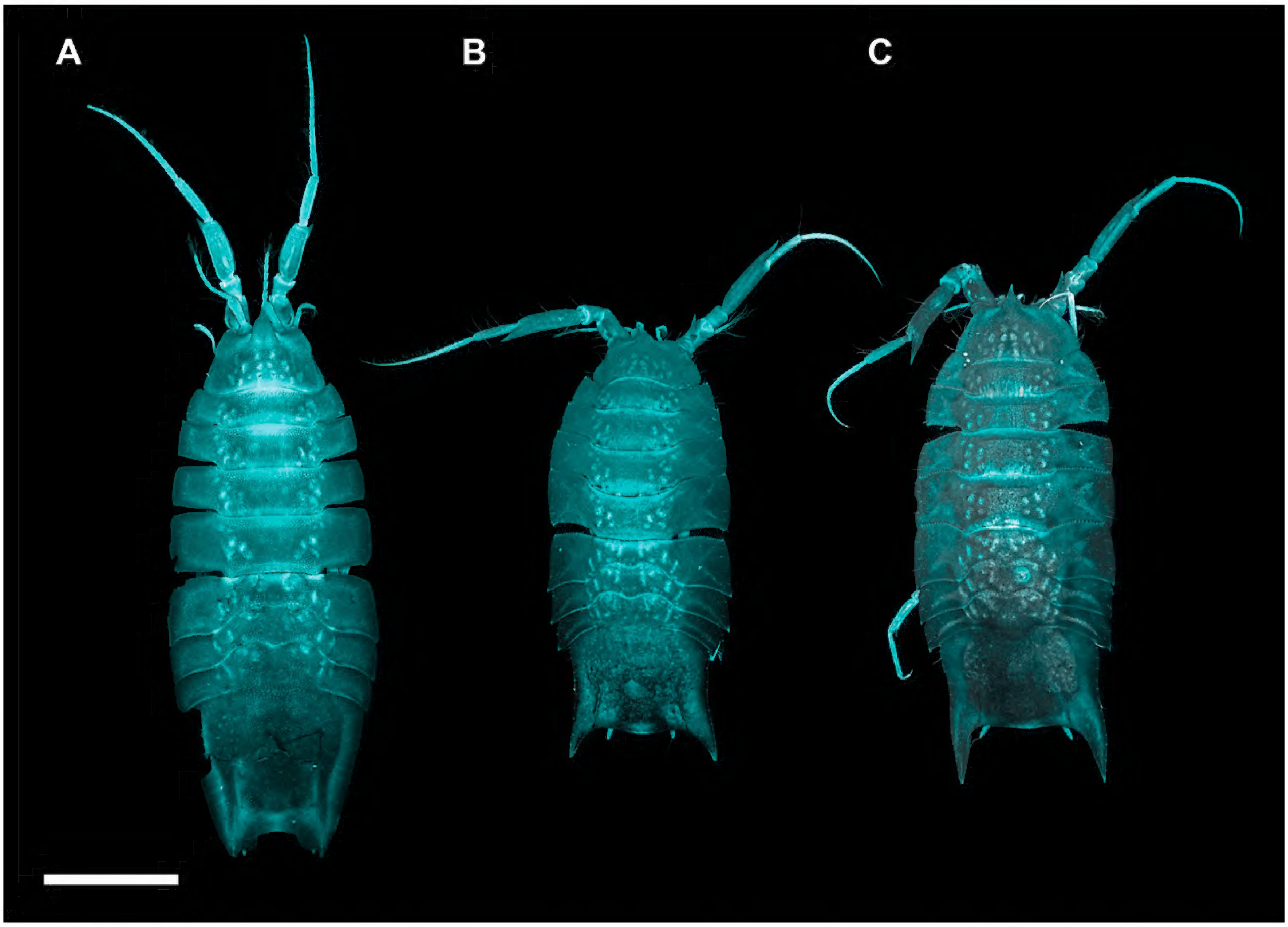

Figure 1. Morphological plasticity of adult males within the *Haploniscus belyaevi* species complex from Knauber et al. (2022). Dorsal habitus CLSM scans of *H. hades* sp. nov. (**A**), *H. belyaevi* (**B**), and *H. erebus* sp. nov. (**C**). Scale bar: 1 mm.

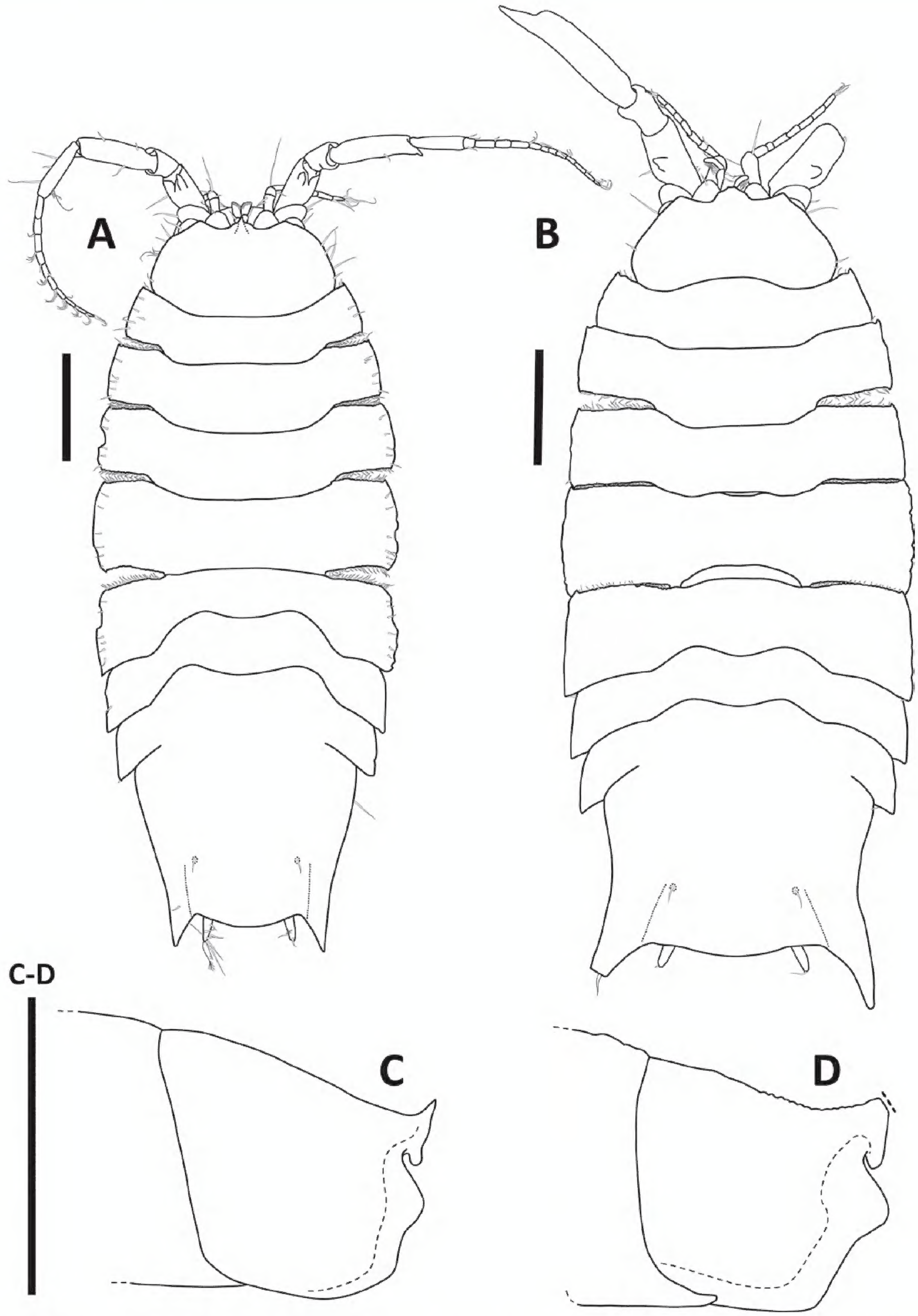

Figure 2. *Haploniscus belyaevi* Birstein, 1963 female paraneotype SKB Hap24 (**A, C**); male neotype, SKB Hap46 (**B, D**). **A, B.** Habitus, dorsal view; **C, D.** Head, lateral view. Scale bars: 0.5 mm.

and a male neotype alongside additional paratypes were assigned from recent material of the SokhoBio expedition (compare *H.* SO-KIR from Knauber et al. 2022), which exhibit a strong morphological resemblance to *H. belyaevi* as featured in the original description. This goes alongside the designation of a type locality, which is in the vicinity of a "Vityaz" station, where *H. belyaevi* was historically sampled.

Type locality. LV71–09–07, RV "Akademik M. A. Lavrentyev", SokhoBio expedition, EBS, 3374 m, 46°12.2'N, 152°03.1'E, Northwest Pacific, abyssal branch of the Kuril-Kamchatka Trench into the Bussol Strait.

Further records. St. LV71–01–08: SKB Hap25 (manca) MIMB 50295; St. LV71–04–09: SKB Hap39 (manca) SMF 56556, SKB Hap42 (manca) MIMB 50297, SKB Hap43 (manca) MIMB 50298, SKB Hap60 (adult

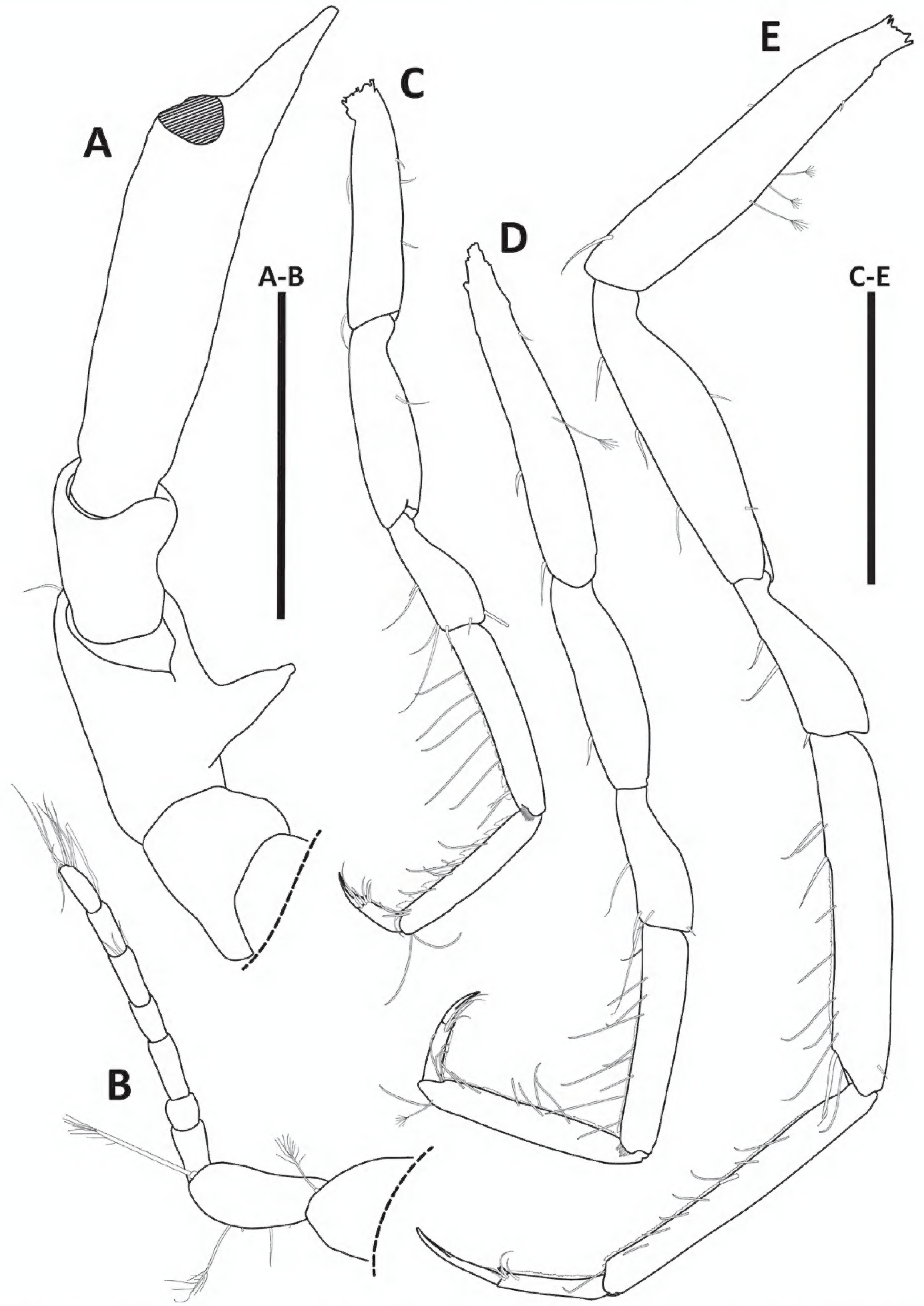

Figure 3. *Haploniscus belyaevi* Birstein, 1963 male neotype, SKB Hap46. **A.** Antenna II; **B.** Antenna I; **C.** Pereopod I; **D.** Pereopod II; **E.** Pereopod VI. Scale bars: 0.4 mm.

female) MIMB 50305, SKB Hap61 (adult female) MIMB 50306; St. LV71–04–10: SKB Hap07 (adult male) SMF 56524, SKB Hap17 (adult female) SMF 56534, SKB Hap38 (manca) SMF 56555; St. LV71–07–03: SKB Hap12 (manca) SMF 56529, SKB Hap19 (adult male) SMF 56536, SKB Hap20 (manca) MIMB 50293, SKB Hap56 (adult male) MIMB 50302, SKB Hap57 (adult female) SMF 56574, SKB Hap58 (adult male) MIMB 50303, SKB Hap59 (adult male) MIMB 50304; St. LV71–07–04: SKB Hap03 (adult female) MIMB 50292, SKB Hap40 (adult female) MIMB 50296, SKB Hap41 (adult female) SMF 56558, SKB Hap44 (manca) MIMB 50299, SKB Hap45 (manca) SMF 56562; St. LV71–09–06: SKB Hap15 (manca) SMF 56532, SKB Hap23 (adult female) SMF 56540; St. LV71–09–07: SKB Hap05 (adult male) SMF 56522, SKB Hap16 (manca) SMF 56533,

Figure 4. *Haploniscus belyaevi* Birstein, 1963 male neotype, SKB Hap46. **A.** Maxillipeds; **B.** Right mandible; **C.** Left mandible; **D.** Maxilla II; **E.** Maxilla I; **F.** Maxillipeds, detail of distomedial margins of endites; **G.** Left mandible, detail of incisor, *lacinia mobilis*, and molar process; **H.** Right mandible, detail of incisor and molar process. Scale bars: 0.1 mm.

SKB Hap32 (adult male) SMF 56549, SKB Hap33 (manca) SMF 56550, SKB Hap47 (adult male) MIMB 50301.

Distribution. Northwest Pacific, Sea of Okhotsk, Kuril Basin, and abyssal regions to the northwest of the Kuril-Kamchatka Trench, depth 3299–3386 m. Given its occurrence on both sides of the Kuril Island Ridge, it might be possible that this species' lowest bathymetric limit might lie even shallower, as it most likely dispersed across the Bussol Strait in one or other direction with a maximum depth of 2,350 m. The original species description of *H. belyaevi* depicts a distributional range extending far into the KKT area, yet despite sampling these areas during the above-mentioned expeditions, *H. belyaevi* was solely recorded in the vicinity of the Bussol Strait. One can therefore only hypothesize that Birstein, potentially due to limited material, lumped the distributional patterns

Figure 5. *Haploniscus belyaevi* Birstein, 1963 male neotype, SKB Hap46. **A.** Pleopod I; **B.** Pleopod II, ventral view; **C.** Pleopod II, dorsal view; **D.** Pleopod III; **E.** Pleopod IV; **F.** Pleopod V. Scale bar: 0.25 mm.

of multiple *belyaevi*-complex members together, not realizing that he was dealing with multiple species. Visualized in Fig. 27.

Synonymy. *Haploniscus* SO-KIR (see Knauber et al. 2022).

Diagnosis. The species differs from other members of the *belyaevi*-complex in the following characters: rostrum curved upwards, anteriorly flat; Prn 1 anterior tergite margin delicately serrated, setose; Prn 1 anterolateral angles with minute acute projection; posterolateral processes short, more than 0.10 Plt length, curved in males, oriented posteriorly.

Molecular diagnosis. Differing in the 16S gene from other species of the *belyaevi*-complex in the nucleotide C (position 249 of the alignment) as well as the nucleotides G (199), C (334), T (376), C (409), A (412), and G (592) of the COI gene.

Description. Male. ***Body*** (Figs 1B, 2B) length 2.3 width; subrectangular; anterior body length (Ceph–Prn 4) 1.0 posterior body length (Prn 5–Plt); lateral margin interrupted between Prn 7 and Plt, otherwise continuous.

Cephalothorax (Figs 1B, 2B, D) length 0.38 width, 0.10 body length, width 0.58 body width; frontal margin width 0.50 Ceph width; rostrum curved upwards, frontally plane.

Pereonite 1 (Figs 1B, 2B) anterior tergite margin through Prn 5 anterior tergite margin delicately serrated, setose; Prn 1–5 anterolateral angles slightly projecting; Prn 1–4 posterolateral angles slightly projecting; Prn 4 lateral margin length 1.04 Prn 5 lateral margin length.

Pleotelson (Figs 1B, 2B, 26H) length 0.74 width, 0.25 body length, rectangular, posterior margin rounded, convex; tergite surface smooth; with posterolateral

tergal ridge between uropod insertion and posterolateral process; posterolateral processes short, 0.31 Plt length, curved, oriented posteriorly.

Antenna I (Fig. 3B) length 0.17 body length; flagellum with 5 articles.

Antenna II (Fig. 3A) length 0.31 body length (without missing peduncular article 6 and flagellum); article 3 dorsal projection triangular, projection length 0.30 article 3 length; article 5 projection length 0.28 article 5 length; flagellum with 17 articles (inferred from male paratype).

Mandible (Fig. 4B, C) incisor with 5 cusps, left Md *lacinia mobilis* with 4 cusps.

Maxillipeds (Fig. 4A) with 3 coupling hooks each.

Pereopod I (Fig. 3C) length 0.40 body length. **PII** (Fig. 3D) length 0.49 body length. **PIII** length 0.53 body length. **PIV** length 0.53 body length. **PV** length 0.64 body length. **PVI** (Fig. 3E) length 0.71 body length; P lengths gradually increasing from PI to PVI, PVII shorter than PVI.

Pleopod I (Figs 5A, 26H) medial lobes subtriangular, projecting caudolaterally; separated at the apex by a narrow gap.

Pleopod II (Fig. 5B, C) protopod semi-circular, with distal lobe extending beyond protopod distal margin; endopod stylet 1.6 protopod length.

Female. Differs from male in the following characters:

Body (Fig. 2A) length 2.3 width; oval; anterior body length (Ceph–Prn 4) 0.95 posterior body length (Prn 5–Plt).

Cephalothorax (Fig. 2A, C) length 0.48 width, 0.13 body length, width 0.60 body width; frontal margin width 0.47 Ceph width.

Pereonite (Fig. 2A) 4 lateral margin length 1.05 Prn 5 lateral margin length.

Pleotelson (Figs 2A, 26G) length 0.83 width, 0.27 body length, trapezoidal; posterolateral processes 0.20 Plt length, straight.

Antenna I (Fig. 2A) length 0.16 body length; flagellum with 4 articles.

Antenna II (Fig. 2A) length 0.57 body length; flagellum with 12 articles.

Operculum (Fig. 26G) Length 1.0 width, 0.77 Plt length; distal margin with numerous, evenly distributed long setae.

Haploniscus apaticus Knauber & Riehl, sp. nov.

https://zoobank.org/2E90065E-FCEE-470C-9AE0-B173281E7677

Figs 6–9, 26

Holotype. SKB Hap08, adult male (stage VI), 3.3 mm, MIMB 50307.

Paratypes. SKB Hap18, adult female (stage IV), 3.2 mm, MIMB 50308; SKB Hap48, adult female (stage IV; genome), SMF 56565.

Type locality. St. LV71–04–10, RV "Akademik M. A. Lavrentyev", SokhoBio expedition, EBS, 3366 m, 47°12.2'N, 149°36.7'E, Northwest Pacific, Sea of Okhotsk, Kuril Basin.

Further records. St. LV71–02–07: SKB Hap27 (manca) SMF 56544, SKB Hap36 (manca) MIMB 50309; St. LV71–04–09: SKB Hap55 (manca) MIMB 50310, SKB Hap62 (adult male) SMF 56579; St. LV71–10–07: SKB Hap02 (adult female) SMF 56519.

Distribution. Northwest Pacific, Sea of Okhotsk, Kuril Basin, depth 3351–3366 m. Visualized in Fig. 27.

Etymology. "*apaticus*" is a Latinized adjective derived from "Apate", the goddess of deceit in Greek mythology. This name refers to this species' lack of a pronounced sexual dimorphism, e.g., in the pleotelson shape, and overall inconspicuous morphology, keeping it hidden amongst its sibling species until recently. *Haploniscus apaticus* can be interpreted in English as "deceitful or deceptive *Haploniscus*."

Synonymy. *Haploniscus* SO-SO (see Knauber et al. 2022).

Diagnosis. Differs from other species of the *belyaevi*-complex in the following characters: Prn 4 lateral margin longer than Prn 5 lateral margin; Plt posterolateral processes straight, oriented posterolaterally; PV–VII lengths distinctly exceeding PI–IV lengths.

Molecular diagnosis. differing in the COI gene from other species of the *belyaevi*-complex in the nucleotides T (position 69 of the alignment), A (220), A (364), G (412), G (469), A (475), and C (556).

Description. Male. ***Body*** (Fig. 6B) length 2.5 width; oval; anterior body length (Ceph–Prn 4) 1.0 posterior body length (Prn 5–Plt); lateral margin interrupted between Prn 7 and Plt, otherwise continuous.

Cephalothorax (Fig. 6B, D) length 0.41 width, 0.10 body length, width 0.59 body width; frontal margin width 0.48 Ceph width; rostrum curved upwards.

Pereonite 1 (Fig. 6B) posterior tergite margin through Prn 5 anterior tergite margin delicately serrated, setose; Prn 2–5 anterolateral angles slightly projecting; Prn 1–4 posterolateral angles slightly projecting; Prn 4 lateral margin length 1.17 Prn 5 lateral margin length.

Pleotelson (Figs 6B, 26J) length 0.79 width, 0.25 body length, trapezoidal, posterior margin rounded, convex; tergite surface smooth; with posterolateral tergal ridge between uropod insertion and posterolateral process; posterolateral processes short, 0.35 Plt length, straight, oriented posterolaterally.

Antenna I (Fig. 7E) length 0.16 body length; flagellum with 5 articles.

Antenna II (Fig. 7A) length 0.69 body length; article 3 dorsal projection triangular, projection length 0.38 article 3 length; article 5 projection length 0.43 article 5 length; flagellum with 19 articles.

Mandible (Fig. 8B, C) incisor with 5 cusps, left Md *lacinia mobilis* with 4 cusps.

Maxillipeds (Fig. 8A) left Mxp with 4 coupling hooks; right Mxp with 3 coupling hooks.

Pereopod II (Fig. 7C) length 0.34 body length. **PIII** length 0.35 body length. **PIV** length 0.37 body length.

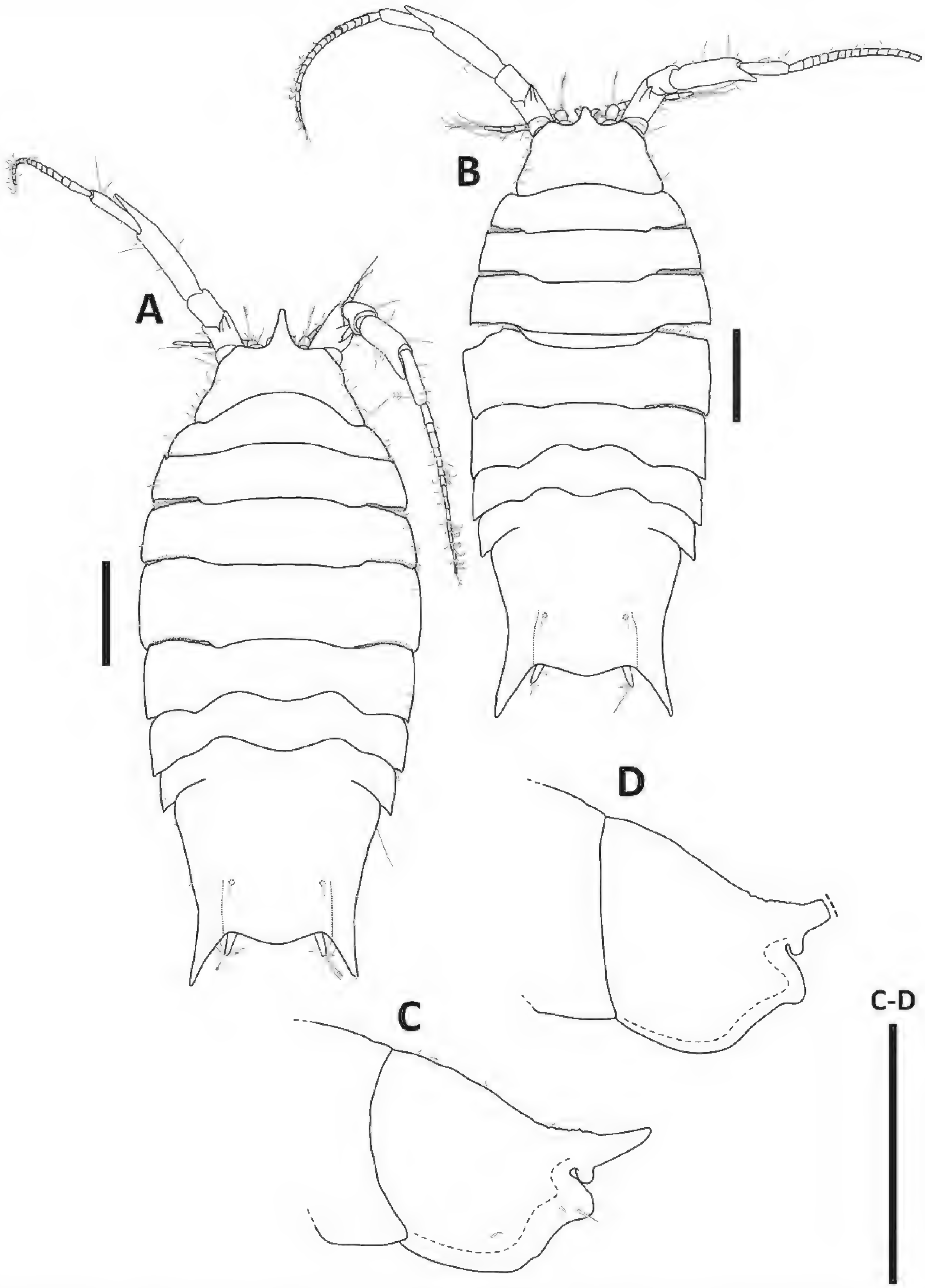

Figure 6. *Haploniscus apaticus* sp. nov. female paratype, SKB Hap18 (**A, C**); male holotype SKB Hap08 (**B, D**). **A, B.** Habitus, dorsal view; **C, D.** Head, lateral view. Scale bars: 0.5 mm.

PV length 0.64 body length. **PVI** (Fig. 7D) length 0.68 body length. **PVII** length 0.62 body length; PV–VII lengths distinctly exceeding PI–IV lengths, PVII shorter than PVI.

Pleopod I (Figs 9A, 26J) medial lobes subtriangular, projecting caudolaterally; adjoining at the apex.

Pleopod II (Fig. 9B, C) protopod semi-circular, with distal lobe extending beyond protopod distal margin; endopod stylet 1.8 protopod length.

Female. Differs from male in the following characters:

Body (Fig. 6A) length 2.4 width; anterior body length (Ceph–Prn 4) 0.95 posterior body length (Prn 5–Plt).

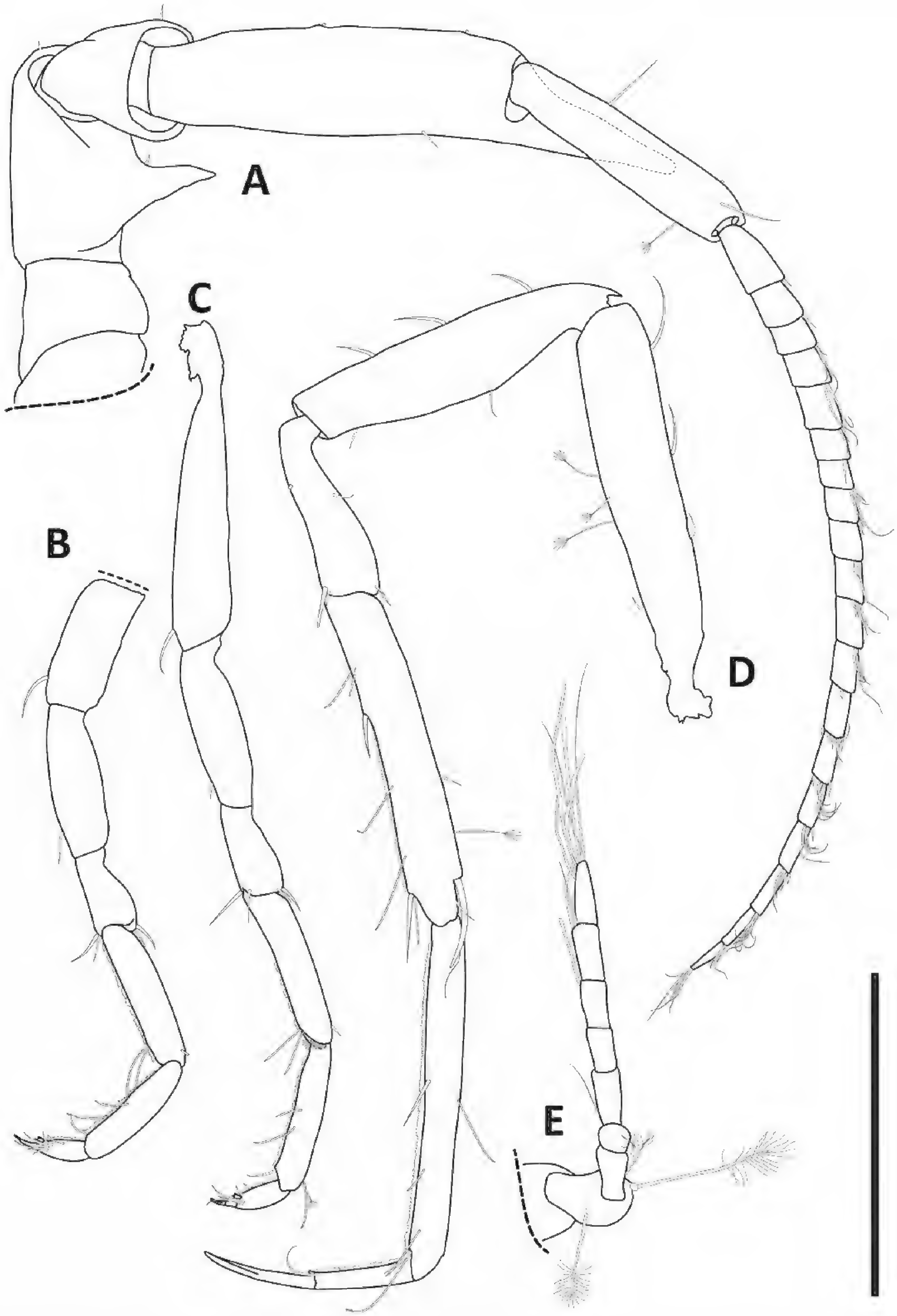

Figure 7. *Haploniscus apaticus* sp. nov. male holotype, SKB Hap08. **A.** Antenna II; **B.** Pereopod I; **C.** Pereopod II; **D.** Pereopod VI; **E.** Antenna I. Scale bar: 0.4 mm.

Cephalothorax (Fig. 6A, C) length 0.26 width, 0.07 body length, width 0.60 body width; frontal margin width 0.51 Ceph width.

Pereonite 4 (Fig. 6A) lateral margin length 1.24 Prn 5 lateral margin length.

Pleotelson (Figs 6A, 26I) length 0.81 width, 0.25 body length; posterolateral processes 0.32 Plt length.

Antenna I (Fig. 6A) length 0.14 body length; flagellum with 4 articles.

Antenna II (Fig. 6A) length 0.63 body length; flagellum with 16 articles.

Operculum (Fig. 26I) length 0.97 width, 0.81 Plt length; distal margin with numerous, evenly distributed long setae; lateral margins with fewer, evenly distributed short setae.

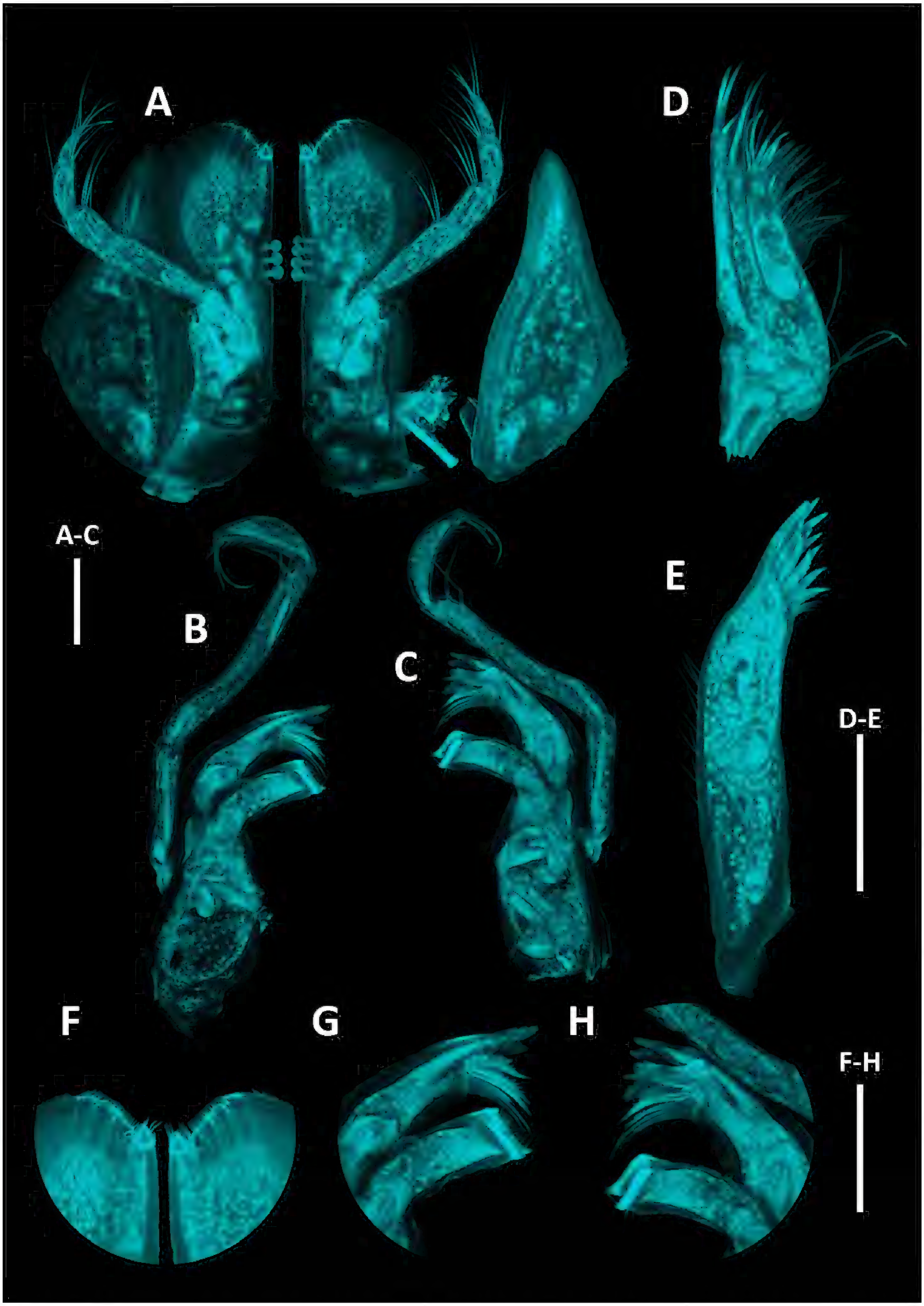

Figure 8. *Haploniscus apaticus* sp. nov. male holotype, SKB Hap08. **A.** maxillipeds; **B.** Right mandible; **C.** Left mandible; **D.** Maxilla II; **E.** Maxilla I; **F.** Maxillipeds, detail of distomedial margins of endites; **G.** Right mandible, detail of incisor and molar process; **H.** Left mandible, detail of incisor, *lacinia mobilis*, and molar process. Scale bars: 0.1 mm.

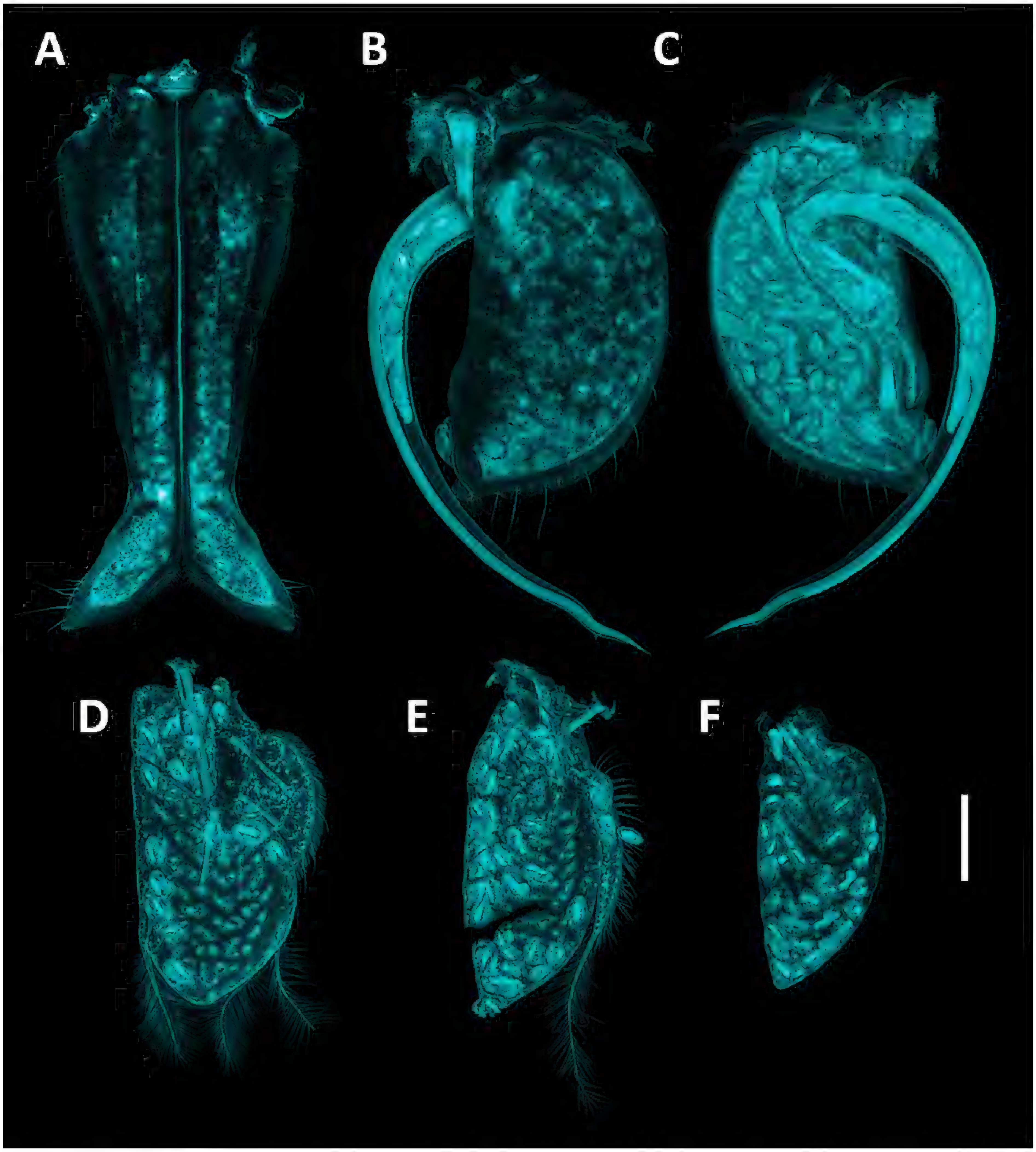

Figure 9. *Haploniscus apaticus* sp. nov. male holotype, SKB Hap08. **A.** Pleopod I; **B.** Pleopod II, ventral view; **C.** Pleopod II, dorsal view; **D.** Pleopod III; **E.** Pleopod IV; **F.** Pleopod V. Scale bar: 0.25 mm.

Haploniscus erebus Knauber & Riehl, sp. nov.

https://zoobank.org/0CA1699A-04CF-4332-A6B8-F9AA1DD108B4

Figs 1, 10–13, 26

Holotype. SKB Hap54, adult male (stage VI), 3.3 mm, MIMB 50317.

Paratypes. SKB Hap49, adult female (stage IV; genome), SMF 56566; SKB Hap50, adult female (stage IV), 3.3 mm, MIMB 50315.

Type locality. St. LV71–02–07, RV “Akademik M. A. Lavrentyev”, SokhoBio expedition, EBS, 3352 m, 46°40.9'N, 147°28.5'E, Northwest Pacific, Sea of Okhotsk, Kuril Basin.

Further records. St. LV71–02–07: SKB Hap26 (manca) MIMB 50312, SKB Hap28 (manca) MIMB 50313; St. LV71–04–09: SKB Hap10 (manca) MIMB 50311; St. LV71–04–10: SKB Hap09 (manca) SMF 56526; St. LV71–11–06: SKB Hap29 (manca) MIMB 50314, SKB Hap30 (manca) SMF 56547, SKB Hap31 (manca) SMF 56548, SKB Hap51 (manca) MIMB 50316, SKB Hap52 (manca) SMF 56569, SKB Hap53 (manca) SMF 56570, SKB Hap63 (manca) SMF 56580.

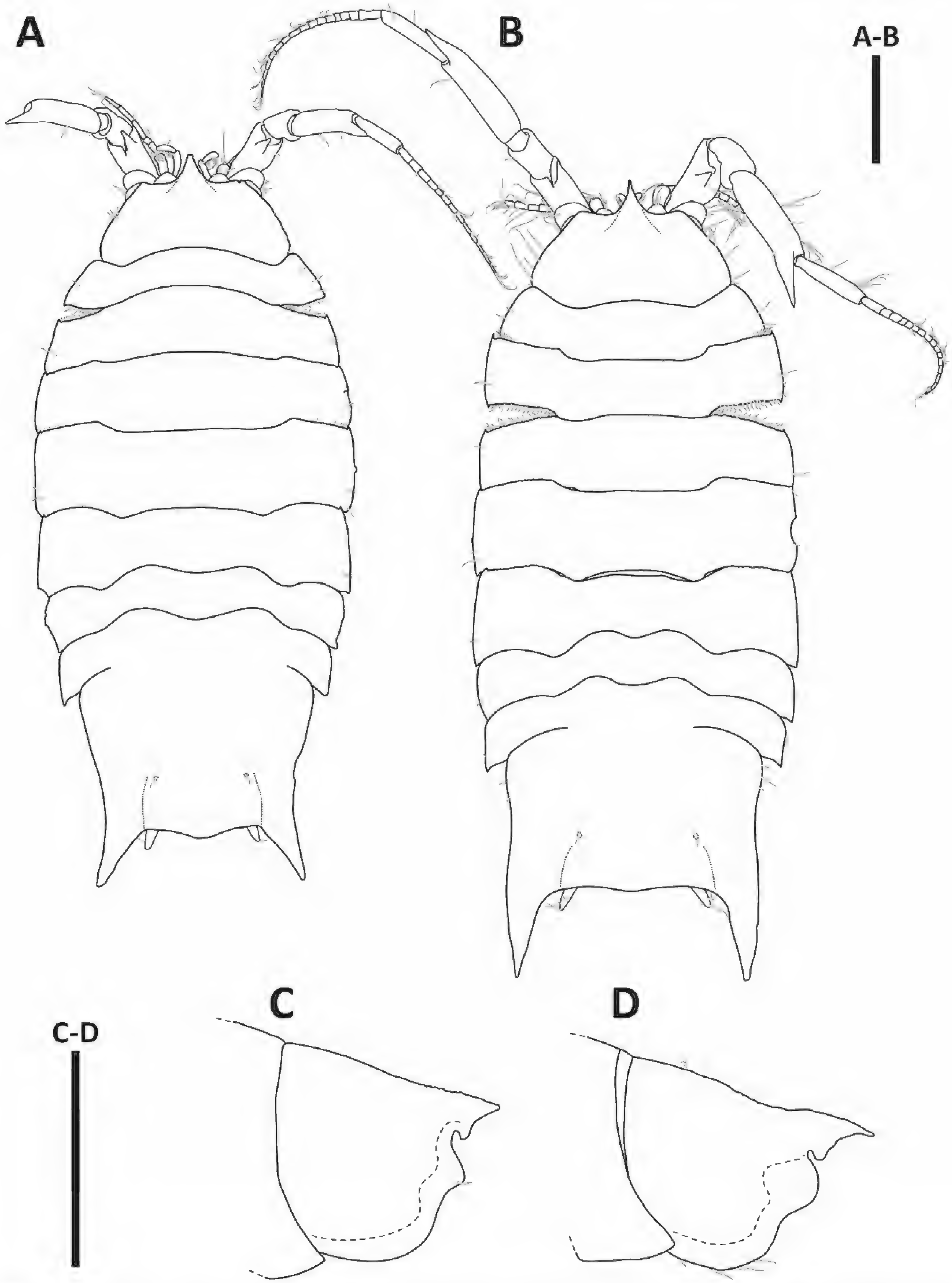

Figure 10. *Haploniscus erebus* sp. nov. female paratype, SKB Hap50 (**A, C**); male holotype SKB Hap54 (**B, D**). **A, B.** Habitus, dorsal view; **C, D.** Head, lateral view. Scale bars: 0.5 mm.

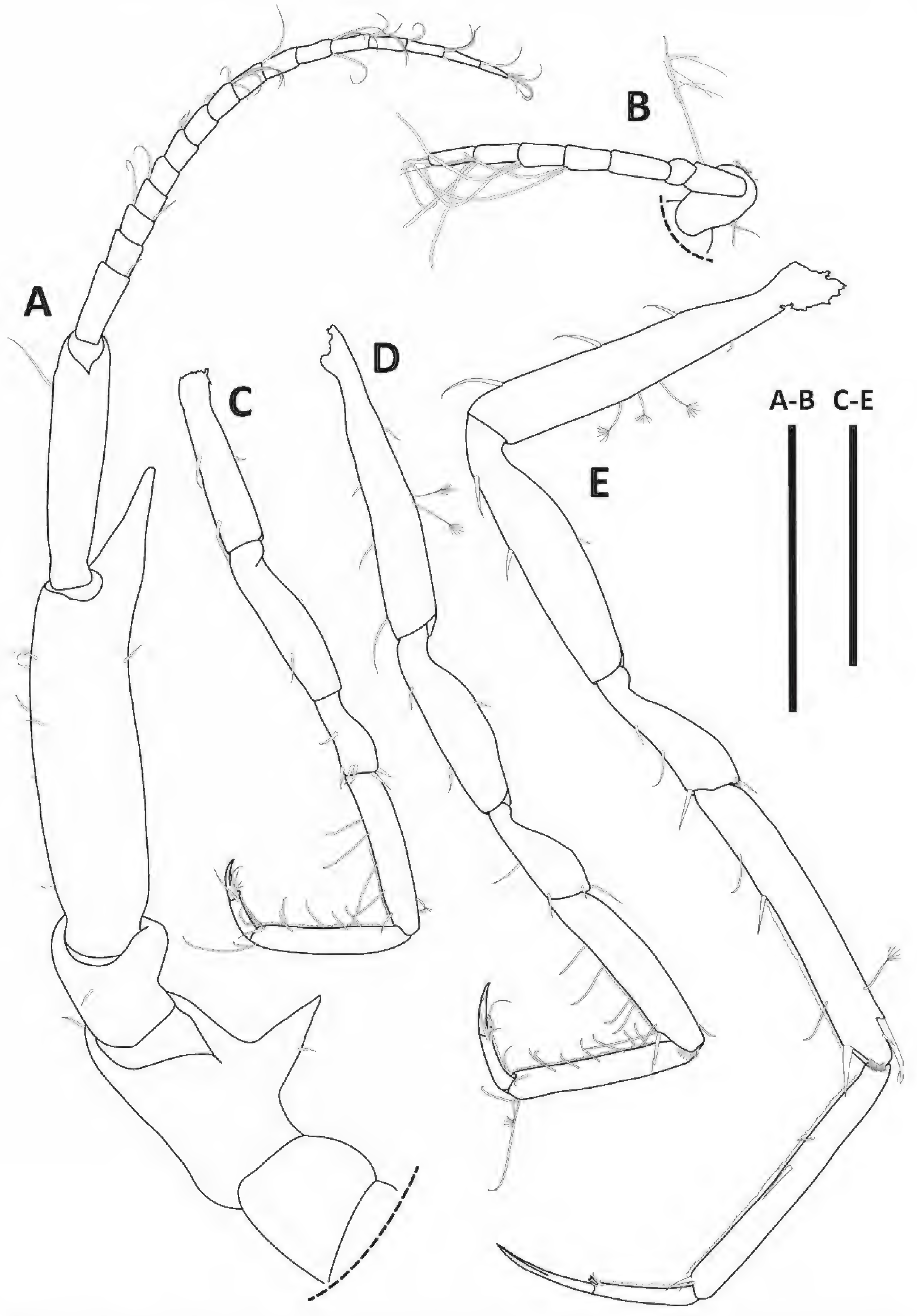

Figure 11. *Haploniscus erebus* sp. nov. male holotype, SKB Hap54. **A.** Antenna II; **B.** Antenna I; **C.** Pereopod I; **D.** Pereopod II; **E.** Pereopod VI. Scale bars: 0.4 mm.

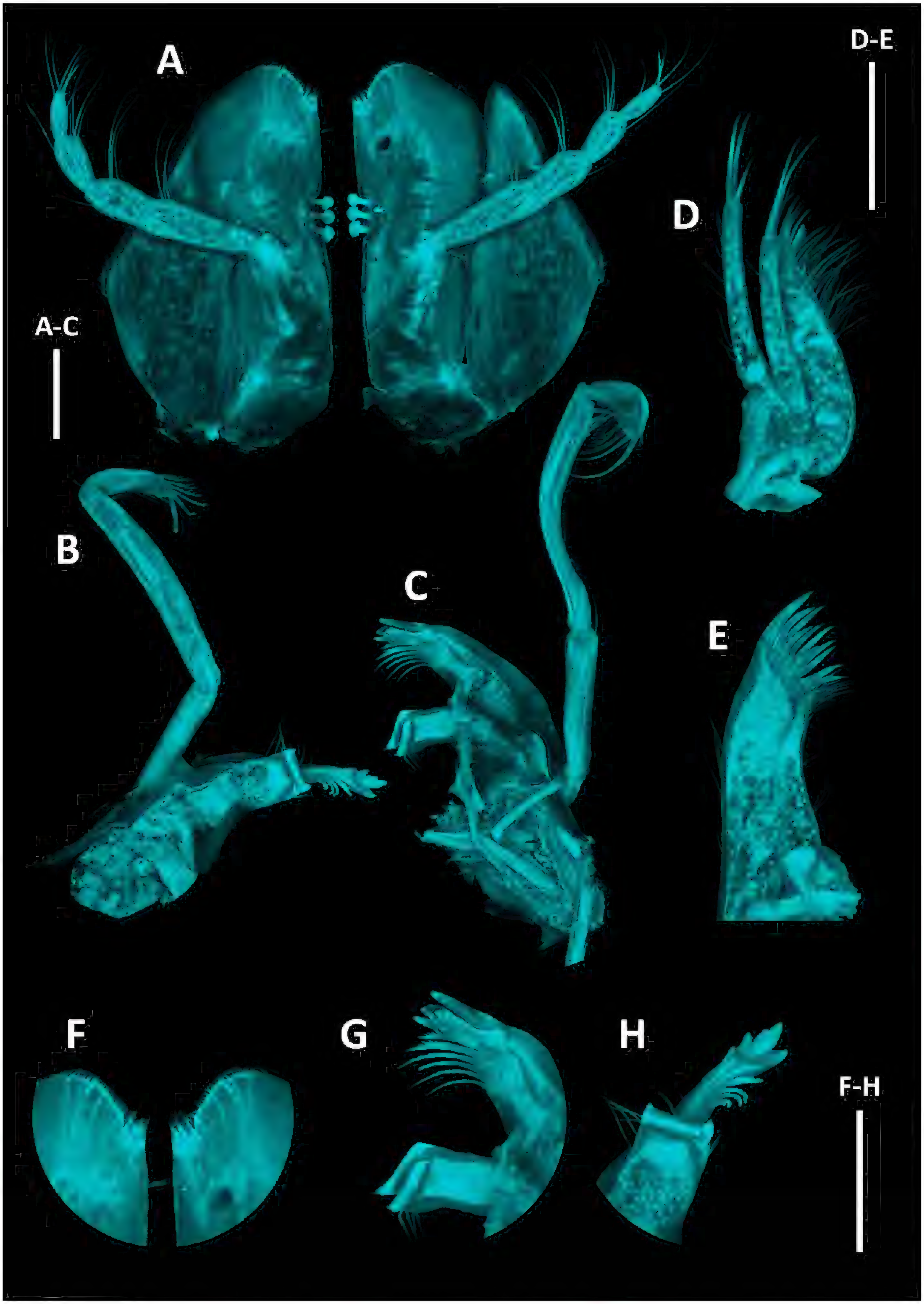

Figure 12. *Haploniscus erebus* sp. nov. male holotype, SKB Hap54. **A.** Maxillipeds; **B.** Right mandible; **C.** Left mandible; **D.** Maxilla II; **E.** Maxilla I; **F.** Maxilliped, right, detail of distomedial margin of endite; **G.** Maxilliped, left, detail of distomedial margin of endite; **H.** Right mandible, detail of incisor and molar process; **I.** Left mandible, detail of incisor, *lacinia mobilis*, and molar process. Scale bars: 0.1 mm.

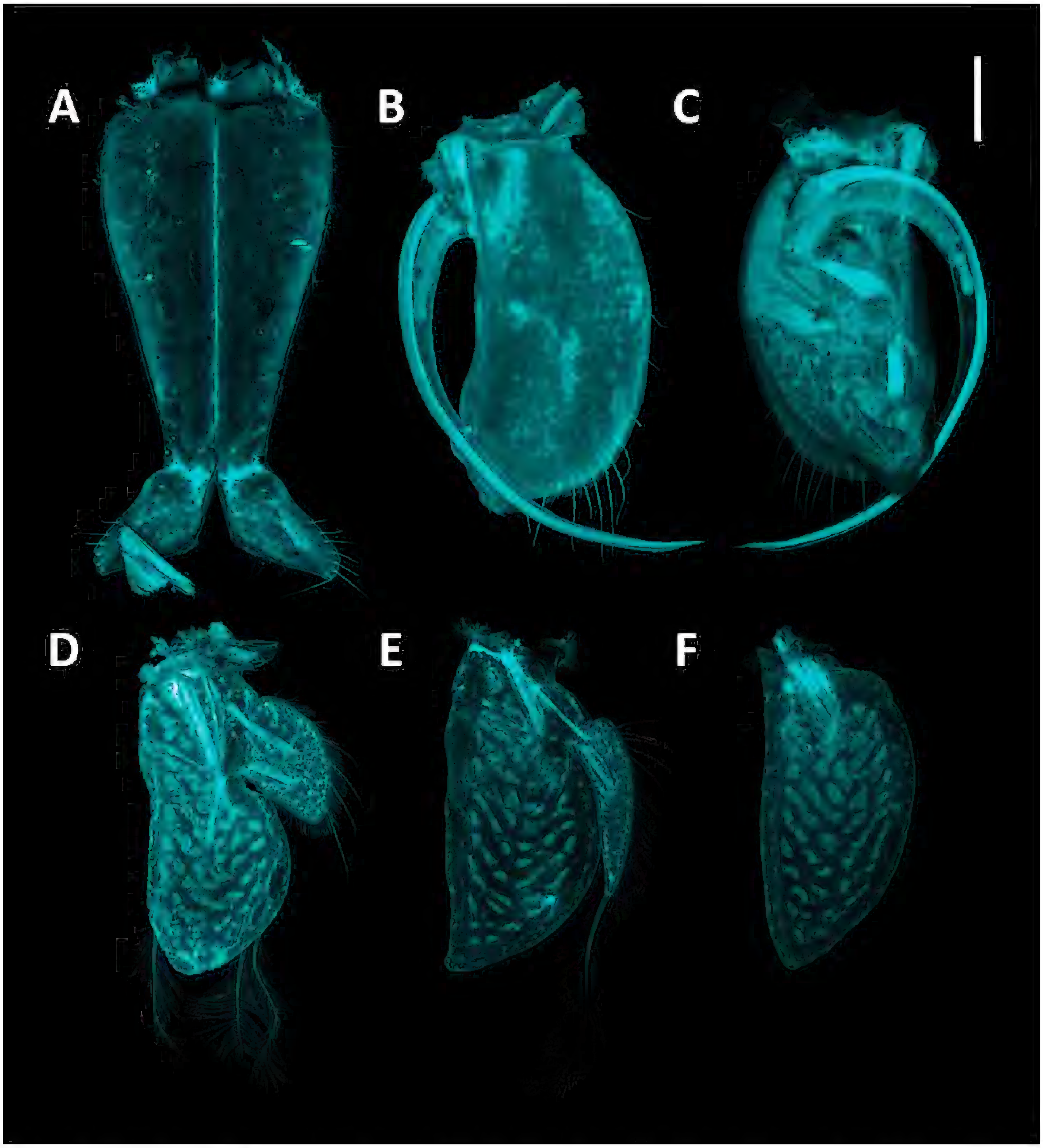

Figure 13. *Haploniscus erebus* sp. nov. male holotype, SKB Hap54. **A.** Pleopod I; **B.** Pleopod II, ventral view; **C.** Pleopod II, dorsal view; **D.** Pleopods III; **E.** Pleopod IV; **F.** Pleopod V. Scale bar: 0.25 mm.

Distribution. Northwest Pacific, Sea of Okhotsk, Kuril Basin, depth 3210–3366 m. Visualized in Fig. 27.

Etymology. From "Erebus" (Ancient Greek: Ἔρεβος), the Greek mythological personification of darkness. It is a noun in apposition.

Synonymy. *Haploniscus* aff. *belyaevi* (see Knauber et al. 2022).

Diagnosis. *Haploniscus erebus* sp. nov. differs from other species of the *belyaevi*-complex in the following characters: rostrum straight, near triangular in lateral view; Plt shape rectangular, posterior margin straight in males; posterolateral processes long, more than 0.50 Plt length in males, straight, oriented posteriorly.

Molecular diagnosis. Differing in the 16S gene from other species of the *belyaevi*-complex in the nucleotides G (position 56 of the alignment), G (64), T (66), G (71), - (150), A (155), T (156), A (204), G (206), C (243), C (342), A (350), G (355), and C (358) as well as the nucleotides T (151), T (154), T (268), T (284), A (286), C (301), G (313), T (352), G (376), C (385), C (388), T (418), A (436), T (451), G (472), G (475), G (502), G (562), and G (565) of the COI gene.

Description. Male. ***Body*** (Figs 1C, 10B) length 2.2 width; subrectangular; anterior body length (Ceph–Prn 4) 1.1 posterior body length (Prn 5–Plt); lateral margin interrupted between Prn 7 and Plt, otherwise continuous.

Cephalothorax (Figs 1C, 10B, D) length 0.45 width, 0.13 body length, width 0.61 body width; frontal margin width 0.50 Ceph width; rostrum straight, near triangular laterally.

Pereonite 1 (Figs 1C, 10B) posterior tergite margin through Prn 5 anterior tergite margin delicately serrated, setose; Prn 2–5 anterolateral angles slightly projecting; Prn 2–4 posterolateral angles slightly projecting; Prn 4 lateral margin length 0.89 Prn 5 lateral margin length.

Pleotelson (Figs 1C, 10B, 26B) length 0.64 width, 0.23 body length, rectangular, posterior margin straight; tergite surface smooth; with posterolateral tergal ridge between uropod insertion and posterolateral process; posterolateral processes long, 0.53 Plt length, straight, oriented posteriorly.

Antenna I (Fig. 11B) length 0.18 body length; flagellum with 6 articles.

Antenna II (Fig. 11A) length 0.68 body length; article 3 dorsal projection triangular, projection length 0.42 article 3 length; article 5 projection length 0.28 article 5 length; flagellum with 16 articles.

Mandible (Fig. 12B, C) incisor with 5 cusps, left Md *lacinia mobilis* with 5 cusps.

Maxillipeds (Fig. 12A) with 3 coupling hooks each.

Pereopod I (Fig. 11C) length 0.43 body length. **PII** (Fig. 11D) length 0.49 body length. **PIII** length 0.58 body length. **PIV** length 0.60 body length. **PV** length 0.75 body length. **PVI** (Fig. 11E) length 0.81 body length. **PVII** length 0.79 body length; P lengths gradually increasing from PI to PVI, PVII shorter than PVI.

Pleopod I (Figs 13A, 26B) medial lobes subtriangular, projecting caudolaterally; separated at the apex by a narrow gap.

Pleopod II (Fig. 13B, C) protopod semi-circular, with distal lobe extending beyond protopod distal margin; endopod stylet 1.8 protopod length.

Female. Differs from male in the following characters:

Body (Fig. 10A) length 2.3 width; oval; anterior body length (Ceph–Prn 4) 0.99 posterior body length (Prn 5–Plt).

Cephalothorax (Fig. 10A, C) length 0.36 width, 0.09 body length, width 0.59 body width; frontal margin width 0.55 Ceph width.

Pereonite 4 (Fig. 10A) lateral margin length 1.0 Prn 5 lateral margin length.

Pleotelson (Figs 10A, 26A) length 0.74 width, 0.24 body length, trapezoidal, posterior margin rounded, convex; posterolateral processes short, 0.34 Plt length, oriented posterolaterally.

Antenna I (Fig. 10A) length 0.14 body length; flagellum with 4 articles.

Antenna II (Fig. 10A) length 0.61 body length; flagellum with 13 articles.

Operculum (Fig. 26A) length 0.93 width, 0.81 Plt length; distal margin with numerous, evenly distributed long setae; lateral margins with fewer, evenly distributed short setae.

Haploniscus hades Knauber & Riehl, sp. nov.

https://zoobank.org/07F6AD09-20C0-4726-B3B7-774BCFC5785F

Figs 1, 14–17, 26

Holotype. KBII Hap137, adult male (stage VI), 3.7 mm, SMF 56419.

Paratypes. KBII Hap104, adult female (stage IV; genome), SMF 56388; KBII Hap213, adult female (stage IV), 2.4 mm, SMF 56495.

Type locality. St. SO250–042, RV "Sonne", KuramBio II expedition, EBS, 7123 m, 45°39.62'N, 152°56.39'E, Northwest Pacific, hadal Kuril-Kamchatka Trench near Bussol Strait.

Further records. St. SO250–020: KBII Hap116 (adult female) SMF 56399; St. SO250–028: KBII Hap208 (adult male) SMF 56490; St. SO250–030: KBII Hap209 (manca) SMF 56491, KBII Hap210 (adult female) SMF 56492; St. SO250–040: KBII Hap220 (ovigerous female) SMF 56502, KBII Hap221 (ovigerous female) SMF 56503, KBII Hap231 (manca) SMF 56513, KBII Hap232 (manca) SMF 56514; St. SO250–042: KBII Hap105 (manca) SMF 56389, KBII Hap106 (manca) SMF 56390, KBII Hap165 (adult male) SMF 56447, KBII Hap198 (manca) SMF 56480, KBII Hap230 (manca) SMF 56512; St. SO250–086: KBII Hap226 (adult male) SMF 56508; St. SO250–097: KBII Hap201 (manca) SMF 56483, KBII Hap204 (adult male) SMF 56486, KBII Hap205 (adult female) SMF 56487, KBII Hap206 (ovigerous female) SMF 56488, KBII Hap214 (manca) SMF 56496, KBII Hap215 (adult female) SMF 56497, KBII Hap216 (adult male) SMF 56498, KBII Hap217 (adult female) SMF 56499, KBII Hap227 (manca) SMF 56509, KBII Hap233 (manca) SMF 56515, KBII Hap234 (manca) SMF 56516; St. SO250–098: KBII Hap203 (manca) SMF 56485.

Distribution. Northwest Pacific, Kuril-Kamchatka Trench, depth 5493–8191 m. Visualized in Fig. 27.

Etymology. The specific epithet "*hades*" is a noun in apposition derived from "Hades" (Ancient Greek: Ἅιδης), the god and ruler of the underworld in Greek mythology. This name refers to this species distributional range within the hadal depths of the Kuril-Kamchatka Trench and the novel feature of the pleotelson posterior margin tergal plates projecting above the uropods in males. These render the uropods "invisible" from dorsal view, reminiscent of Hades' cap of invisibility.

Synonymy. *Haploniscus* KKT hadal (see Knauber et al. 2022).

Diagnosis. *Haploniscus hades* sp. nov. differs from other species of the *belyaevi*-complex in the following characters: rostrum curved upwards, basally with dorsal bulge in males; Plt with posterolateral tergal ridge on posterolateral process and posterior margin tergal plates projecting above uropods (solely present in sister species *H. kerberos* sp. nov. otherwise); AII article 3 dorsal projection hook-shaped; Plp I distally with hook-shaped projection.

Molecular diagnosis. Differing in the 16S gene from other species of the *belyaevi*-complex in the nucleotide A (position 219 of the alignment) as well as the nucleotides

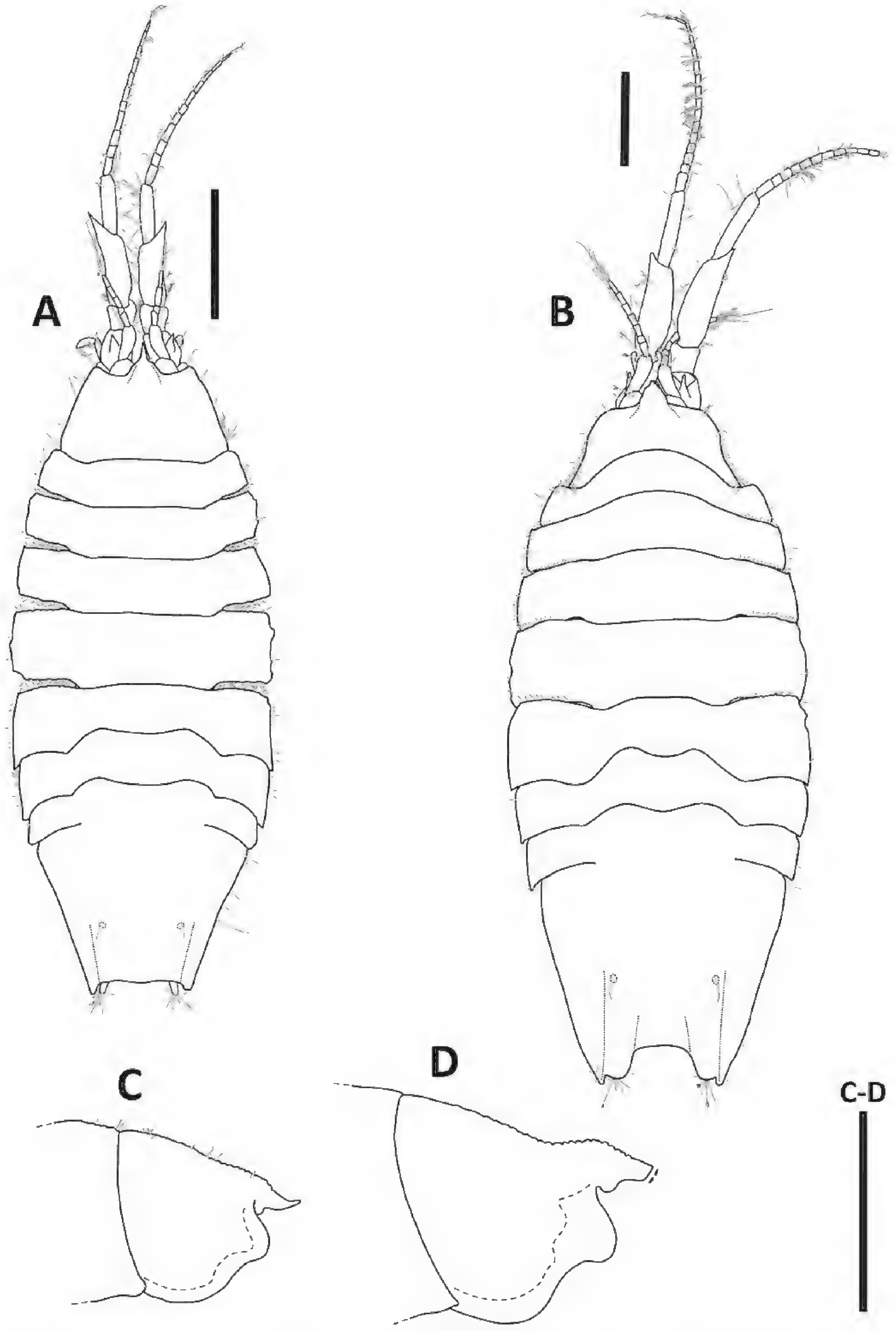

Figure 14. *Haploniscus hades* sp. nov. female paratype, KBII Hap213 (**A, C**); male holotype KBII Hap137 (**B, D**). **A, B.** Habitus, dorsal view; **C, D.** Head, lateral view. Scale bars: 0.5 mm.

G (103), A (211), T (217), C (232), G (256), T (328), A (349), C (364), C (370), C (442), A (469), C (499), and C (571) of the COI gene.

Description. Male. ***Body*** (Figs 1A, 14B) length 2.3 width; oval; anterior body length (Ceph–Prn 4) 0.84 posterior body length (Prn 5–Plt); lateral margin continuous.

Cephalothorax (Figs 1A, 14B, D) length 0.28 width, 0.07 body length, width 0.56 body width; frontal margin width 0.53 Ceph width; rostrum curved upwards, basally with dorsal bulge.

Pereonite 1 (Figs 1A, 14B) posterior tergite margin through Prn 5 anterior tergite margin delicately serrated, setose; Prn 2–4 anterolateral angles slightly projecting; Prn 2–4 posterolateral angles slightly projecting; Prn 4 lateral margin length 0.89 Prn 5 lateral margin length; Prn 5 anterolateral angle not projecting, rectangular.

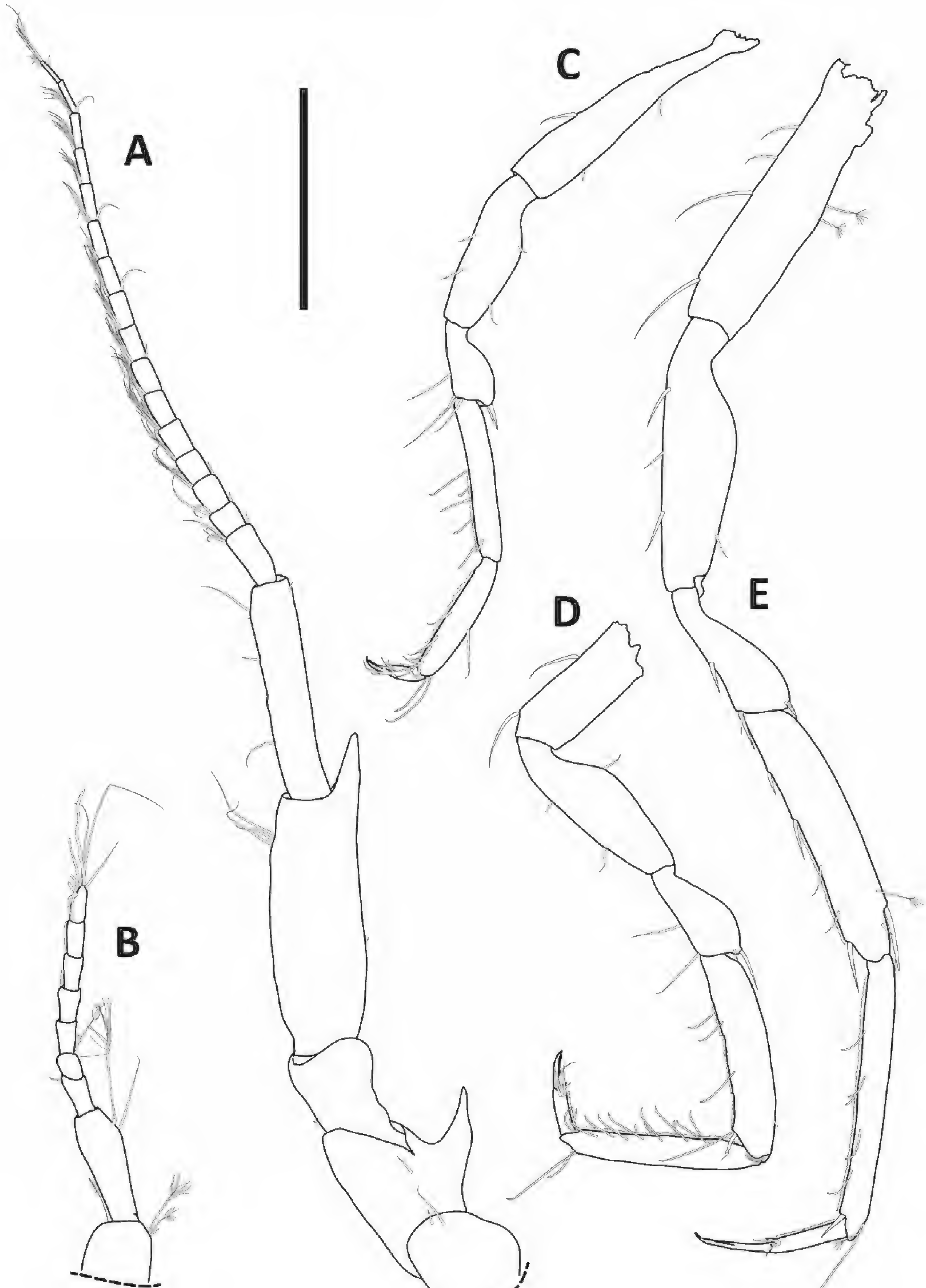

Figure 15. *Haploniscus hades* sp. nov. male holotype, KBII Hap137. **A.** Antenna II; **B.** Antenna I; **C.** Pereopod I; **D.** Pereopod II; **E.** Pereopod VI. Scale bar: 0.4 mm.

Figure 16. *Haploniscus hades* sp. nov. male holotype, KBII Hap137. **A.** Maxillipeds; **B.** Right mandible; **C.** Left mandible; **D.** Maxilla II; **E.** Maxilla I; **F.** Maxillipeds, detail of distomedial margins of endites; **G.** Right mandible, detail of incisor and molar process; **H.** Left mandible, detail of incisor, *lacinia mobilis*, and molar process. Scale bars: 0.1 mm.

Figure 17. *Haploniscus hades* sp. nov. male holotype, KBII Hap137. **A.** Pleopod I; **B.** Pleopod II, dorsal view; **C.** Pleopod II, ventral view; Pleopod III; **D.** Pleopod IV; **E.** Pleopod V. Scale bar: 0.25 mm.

Pleotelson (Figs 1A, 14B, 26F) length 0.75 width, 0.27 body length, trapezoidal, posterior margin concave; tergite surface tuberculate, less distinct than in remaining body; with posterolateral tergal ridge on posterolateral process and posterior margin tergal plates projecting above uropods; posterolateral processes minute, 0.04 Plt length, straight, oriented posteriorly.

Antenna I (Fig. 15B) length 0.17 body length; flagellum with 6 articles.

Antenna II (Fig. 15A) length 0.67 body length; article 3 dorsal projection hook-shaped, projection length 0.39 article 3 length; article 5 projection length 0.26 article 5 length; flagellum with 16 articles.

Mandible (Fig. 16B, C) incisor with 6 cusps, left Md *lacinia mobilis* with 5 cusps.

Maxillipeds (Fig. 16A) with 3 coupling hooks each.

Pereopod I (Fig. 15C) length 0.41 body length. **PIII** length 0.53 body length. **PIV** length 0.54 body length. **PV** length 0.67 body length. **PVI** (Fig. 15E) length 0.70 body length. **PVII** length 0.69 body length; P lengths gradually increasing from PI to PVI, PVII shorter than PVI.

Pleopod I (Figs 17A, 26F) medial lobes convexly rounded, tapering to an obtuse point; distally with hook-shaped projection; separated at the apex by a narrow gap.

Pleopod II (Fig. 17B, C) protopod elongated, suboval; endopod stylet 2.0 protopod length.

Female. Differs from male in the following characters:

Body (Fig. 14A) length 2.4 width; anterior body length (Ceph–Prn 4) 1.0 posterior body length (Prn 5–Plt).

Cephalothorax (Fig. 14A, C) length 0.52 width, 0.14 body length, width 0.63 body width; frontal margin width 0.55 Ceph width.

Pereonite 4 (Fig. 14A) lateral margin length 0.93 Prn 5 lateral margin length.

Pleotelson (Figs 14A, 26E) length 0.75 width, 0.25 body length, posterior margin straight; posterolateral processes 0.08 Plt length.

Antenna I (Fig. 14A) length 0.15 body length; flagellum with 4 articles.

Antenna II (Fig. 14A) length 0.70 body length; flagellum with 11 articles.

Operculum (Fig. 26E) length 1.1 width, 0.74 Plt length; distal margin with numerous, evenly distributed long setae; lateral margins with up to 3 short setae each.

Haploniscus kerberos Knauber & Riehl, sp. nov.

https://zoobank.org/29F19A6D-3FCA-4F9E-9454-170905F09E5E

Figs 18–21, 26

Holotype. KBII Hap136, adult male (stage VI), 3.1 mm, SMF 56418.

Paratypes. KBII Hap122, adult female (stage IV; genome), SMF 56405; KBII Hap123, adult female (stage IV), 2.4 mm, SMF 56406.

Type locality. St. SO250–010, RV "Sonne", KuramBio II expedition, EBS, 5120 m, 43°49.43'N, 151°46.96'E, Northwest Pacific, abyssal plains southeast of the Kuril-Kamchatka Trench.

Further records. St. LV71–10–06: SKB Hap13 (manca) MIMB 50318; St. LV71–10–07: SKB Hap01 (ovigerous female) SMF 56518, SKB Hap22 (adult male) SMF 56539, SKB Hap37 (adult male) MIMB 50319; St. SO250–008: KBII Hap200 (manca) SMF 56482, KBII Hap219 (adult female) SMF 56501, KBII Hap229 (manca) SMF 56511; St. SO250–010: KBII Hap119 (adult male) SMF 56402, KBII Hap120 (adult male) SMF 56403, KBII Hap121 (adult female) SMF 56404, KBII Hap135 (ovigerous female) SMF 56417, KBII Hap228 (manca) SMF 56510; St. SO250–065: KBII Hap211 (manca) SMF 56493, KBII Hap212 (manca) SMF 56494; St. SO250–085: KBII Hap222 (adult male) SMF 56504, KBII Hap223 (adult male) SMF 56505, KBII Hap224 (adult male) SMF 56506; St. SO250–087: KBII Hap218 (ovigerous female) SMF 56500, KBII Hap225 (adult male) SMF 56507, KBII Hap235 (ovigerous female) SMF 56517.

Distribution. Northwest Pacific, abyssal regions adjacent to the Kuril-Kamchatka Trench, depth 4469–5755 m. Visualized in Fig. 27.

Etymology. As a noun in apposition, the epithet "*kerberos*" refers to "Kerberos" (Ancient Greek Κέρβερος) from Greek mythology, the creature guarding the gates of the underworld. This name relates to this species' distributional range, which, according to the available data, is limited to the abyssal plains adjacent to the hadal Kuril-Kamchatka Trench.

Synonymy. *Haploniscus* KKT abyssal (see Knauber et al. 2022).

Diagnosis. *Haploniscus kerberos* sp. nov. is highly similar to *H. hades* sp. nov. in also possessing the characteristic Plt shape with posterolateral tergal ridges terminating on the posterolateral processes and the posterior margin tergal plates projecting above the uropods. It differs from its sister species in the following characters: rostrum basally without dorsal bulge in males (basally with dorsal bulge in *H. hades* sp. nov.) and AII article 3 dorsal projection triangular (hook-shaped in *H. hades* sp. nov.).

Molecular diagnosis. differing in the 16S gene from other species of the *belyaevi*-complex in the nucleotides G (position 173 of the alignment) and G (228), as well as the nucleotides T (61), C (91), C (298), G (346), G (430), G (607), T (625), and G (649) of the COI gene.

Description. Male. ***Body*** (Fig. 18B) length 2.5 width; oval; anterior body length (Ceph–Prn 4) 1.1 posterior body length (Prn 5–Plt); lateral margin continuous.

Cephalothorax (Fig. 18B, D) length 0.35 width, 0.08 body length, width 0.59 body width; frontal margin width 0.54 Ceph width; rostrum curved upwards.

Pereonite 1 (Fig. 18B) posterior tergite margin through Prn 5 anterior tergite margin delicately serrated, setose; Prn 2–4 anterolateral angles slightly projecting; Prn 2–4 posterolateral angles slightly projecting; Prn 4 lateral margin length 0.92 Prn 5 lateral margin length; Prn 5 anterolateral angle not projecting, rectangular.

Pleotelson (Figs 18B, 26D) length 0.68 width, 0.22 body length, trapezoidal, posterior margin concave; tergite surface tuberculate, less distinct than in remaining body; with posterolateral tergal ridge on posterolateral process and posterior margin tergal plates projecting above uropods; posterolateral processes minute, 0.09 Plt length, straight, oriented posteriorly.

Antenna I (Fig. 19B) length 0.20 body length; flagellum with 6 articles.

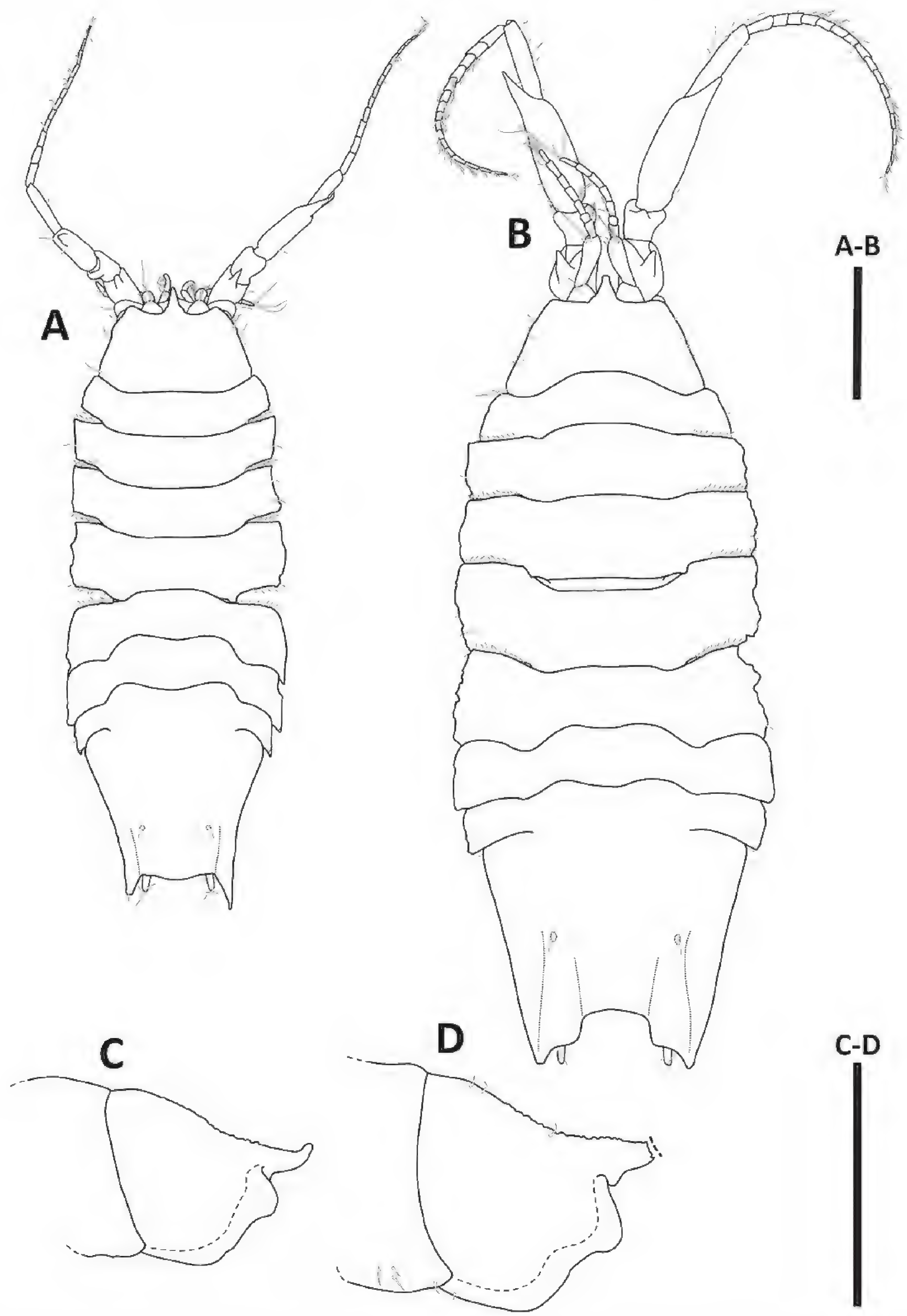

Figure 18. *Haploniscus kerberos* sp. nov. female paratype, KBII Hap123 (**A, C**); male holotype KBII Hap136 (**B, D**). **A, B.** Habitus, dorsal view; **C, D.** Head, lateral view. Scale bars: 0.5 mm.

Antenna II (Fig. 19A) length 0.77 body length; article 3 dorsal projection triangular, projection length 0.31 article 3 length; article 5 projection length 0.22 article 5 length; flagellum with 16 articles.

Mandible (Fig. 20B, C) incisor with 5 cusps, left Md *lacinia mobilis* with 4 cusps.

Maxillipeds (Fig. 20A) with 3 coupling hooks each.

Pereopod I (Fig. 19D) length 0.43 body length. **PVI** (Fig. 19C) length 0.70 body length; P lengths gradually increasing from PI to PVI, PVII shorter than PVI.

Pleopod I missing.

Pleopod II (Fig. 21A, B) protopod elongated, suboval; endopod stylet 2.0 protopod length.

Female. Differs from male in the following characters:

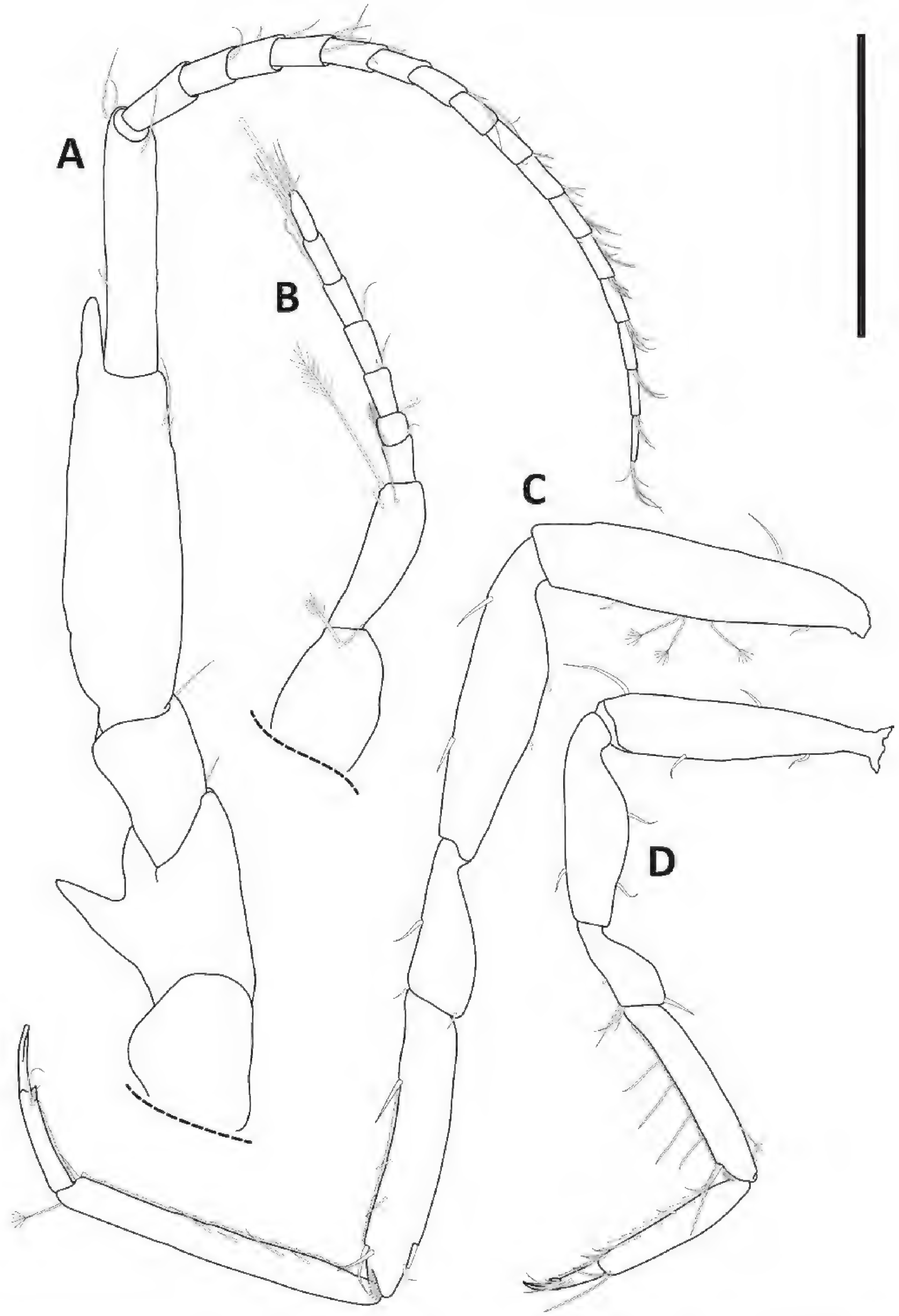

Figure 19. *Haploniscus kerberos* sp. nov. male holotype, KBII Hap136. **A.** Antenna II; **B.** Antenna I; **C.** Pereopod VI; **D.** Pereopod I. Scale bar: 0.4 mm.

Body (Fig. 18A) length 2.7 width; anterior body length (Ceph–Prn 4) 0.94 posterior body length (Prn 5–Plt).

Cephalothorax (Fig. 18A, C) length 0.50 width, 0.12 body length, width 0.66 body width; frontal margin width 0.55 Ceph width.

Pereonite 4 (Fig. 18A) lateral margin length 0.80 Prn 5 lateral margin length.

Pleotelson (Figs 18A, 26C) length 0.84 width, 0.24 body length, posterior margin rounded, convex; with posterolateral tergal ridge between uropod insertion and posterolateral process; posterolateral processes short, 0.23 Plt length.

Antenna I (Fig. 18A) length 0.14 body length; flagellum with 4 articles.

Antenna II (Fig. 18A) length 0.67 body length; flagellum with 12 articles.

Operculum (Fig. 26C) length 1.1 width, 0.75 Plt length; distal margin with numerous, evenly distributed long setae; lateral margins with 2 short setae each.

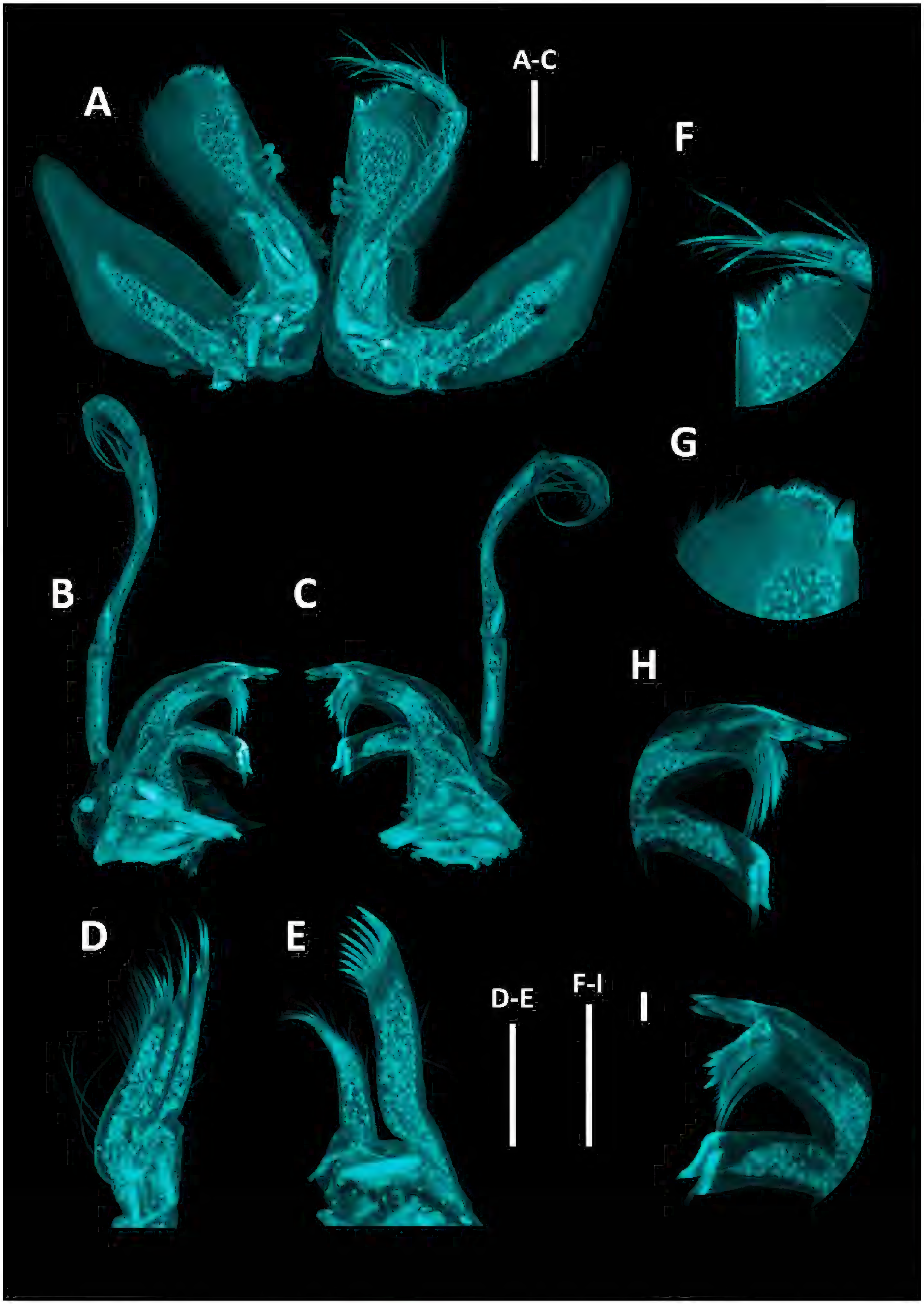

Figure 20. *Haploniscus kerberos* sp. nov. male holotype, KBII Hap136. **A.** Maxillipeds; **B.** Right mandible; **C.** Left mandible; **D.** Maxilla II; **E.** Maxilla I; **F.** Left maxilliped, detail of distomedial margin of endite; **G.** Right maxilliped, detail of distomedial margin of endite; **H.** Right mandible, detail of incisor and molar process; **I.** Left mandible, detail of incisor, *lacinia mobilis*, and molar process. Scale bars: 0.1 mm.

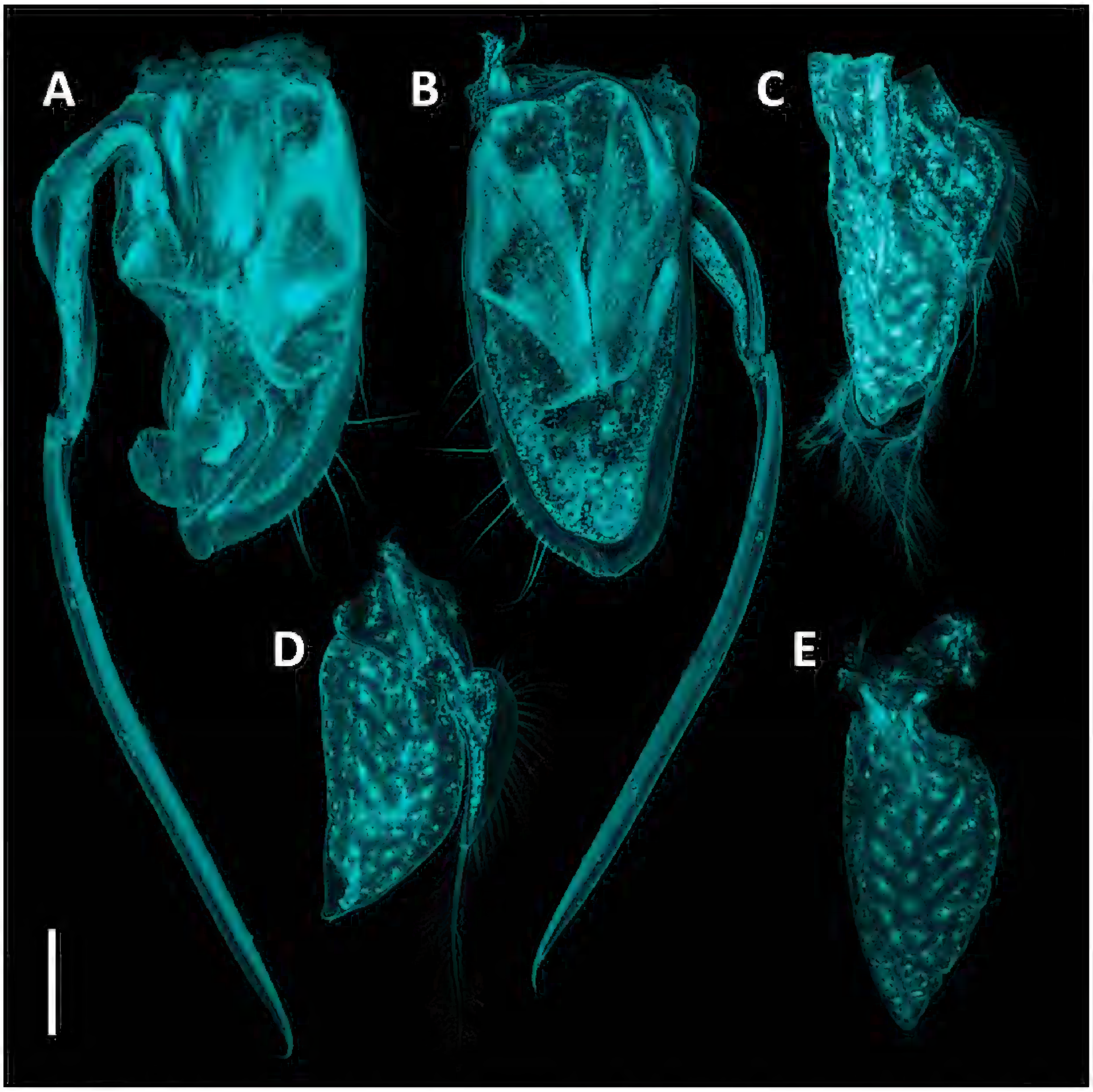

Figure 21. *Haploniscus kerberos* sp. nov. male holotype, KBII Hap136. **A.** Pleopod II, dorsal view; **B.** Pleopod II, ventral view; **C.** Pleopod III; **D.** Pleopod IV; **E.** Pleopod V. Scale bar: 0.25 mm.

Haploniscus nyx Knauber & Riehl, sp. nov.

https://zoobank.org/3AA34260-5C82-45B8-BC35-3779AEE6657E

Figs 22–26

Holotype. SKB Hap34, adult male (stage VI), 3.4 mm, MIMB 50320.

Paratypes. SKB Hap21, adult female (stage IV), 3.0 mm, MIMB 50321.

Type locality. St. LV71–10–07, RV "Akademik M. A. Lavrentyev", SokhoBio expedition, EBS, 4469 m, 46°07.8'N, 152°10.3'E, Northwest Pacific, abyssal branch of the Kuril-Kamchatka Trench into the Bussol Strait.

Further records. St. LV71–10–07: SKB Hap35 (adult male), SMF 56552.

Distribution. Only known from type locality. Northwest Pacific, abyssal region adjacent to the Kuril-Kamchatka Trench to the northwest, depth 4769 m. Visualized in Fig. 27.

Etymology. The epithet "*nyx*," a noun in apposition, is derived from "Nyx" (Ancient Greek Νύξ), the goddess of the night in Greek mythology.

Synonymy. *Haploniscus* SO-WTA (see Knauber et al. 2022).

Diagnosis. *Haploniscus nyx* sp. nov. differs from other species of the *belyaevi*-complex in the following character: pleotelson posterior margin concave in males; Plp I medial lobes convexly rounded, tapering to an obtuse point, distally without a hook-shaped protrusion.

Molecular diagnosis. differing in the 16S gene from other species of the *belyaevi*-complex in the nucleotides G (position 25 of the alignment) and C (312) as well as the nucleotides C (124), G (148), C (193), T (206), C (304), G (334), C (346), G (481), T (496), C (508), C (520), G (553), G (556), and C (628) of the COI gene.

Description. Male. ***Body*** (Fig. 22B) length 2.2 width; subrectangular; anterior body length (Ceph–Prn 4) 0.99 posterior body length (Prn 5–Plt); lateral margin continuous.

Cephalothorax (Fig. 22B, D) length 0.30 width, 0.07 body length, width 0.55 body width; frontal margin width 0.46 Ceph width; rostrum curved upwards.

Pereonite 1 (Fig. 22B) posterior tergite margin through Prn 5 anterior tergite margin delicately serrated, setose;

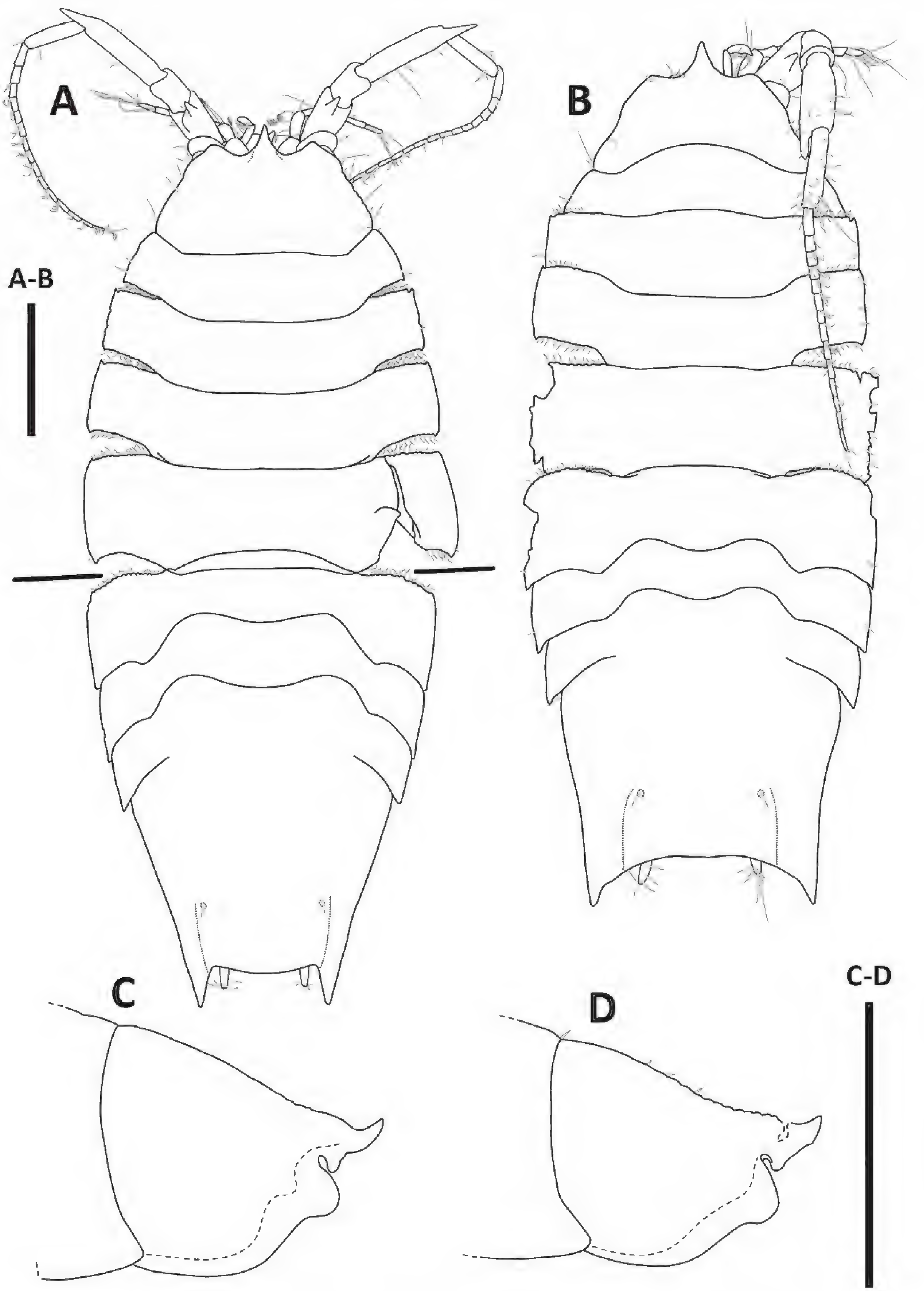

Figure 22. *Haploniscus nyx* sp. nov. female paratype, SKB Hap21 (**A, C**); male holotype SKB Hap34 (**B, D**). **A, B.** Habitus, dorsal view; **C, D.** Head, lateral view. Scale bars: 0.5 mm. Due to pronounced body curvature, the habitus drawing of the female paratype was prepared by two separate drawings, stitching them together along the illustrated line.

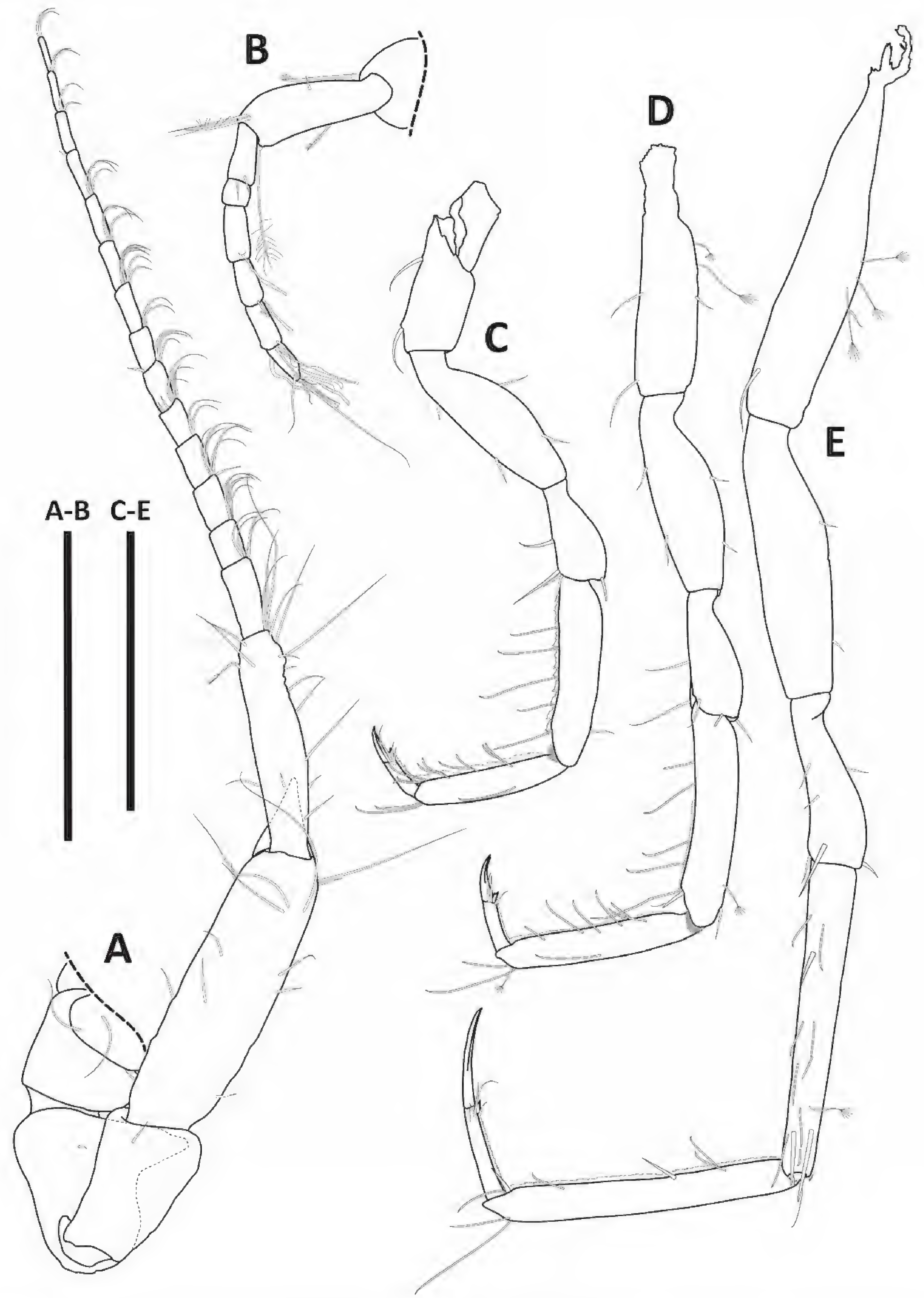

Figure 23. *Haploniscus nyx* sp. nov. male holotype, SKB Hap34. **A.** Antenna II; **B.** Antenna I; **C.** Pereopod I; **D.** Pereopod II; **E.** Pereopod VI. Scale bars: 0.4 mm.

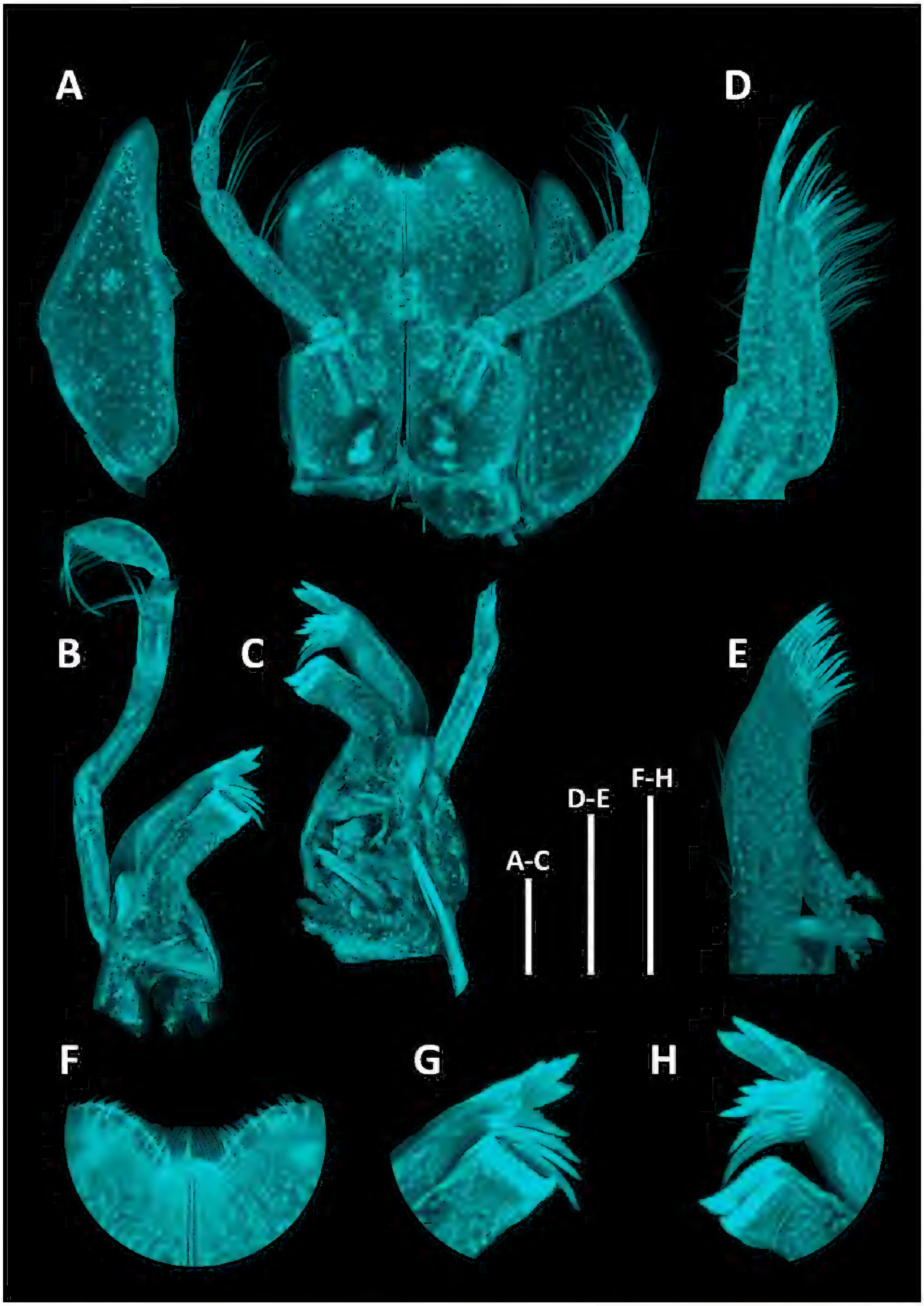

Figure 24. *Haploniscus nyx* sp. nov. male holotype, SKB Hap34. **A.** Maxillipeds; **B.** Right mandible; **C.** Left mandible; **D.** Maxilla II; **E.** maxilla I; **F.** Maxillipeds, detail of distomedial margins of endites; **G.** Right mandible, detail of incisor and molar process; **H.** Left mandible, detail of incisor, *lacinia mobilis*, and molar process. Scale bars: 0.1 mm.

Prn 2–5 anterolateral angles slightly projecting; Prn 1–4 posterolateral angles slightly projecting; Prn 4 lateral margin length 1 Prn 5 lateral margin length.

Pleotelson (Figs 22B, 26L) length 0.72 width, 0.23 body length, trapezoidal, posterior margin concave; tergite surface smooth; with posterolateral tergal ridge between uropod insertion and posterolateral process; posterolateral processes minute, 0.13 Plt length, straight, oriented posteriorly.

Antenna I (Fig. 23B) length 0.16 body length; flagellum with 5 articles.

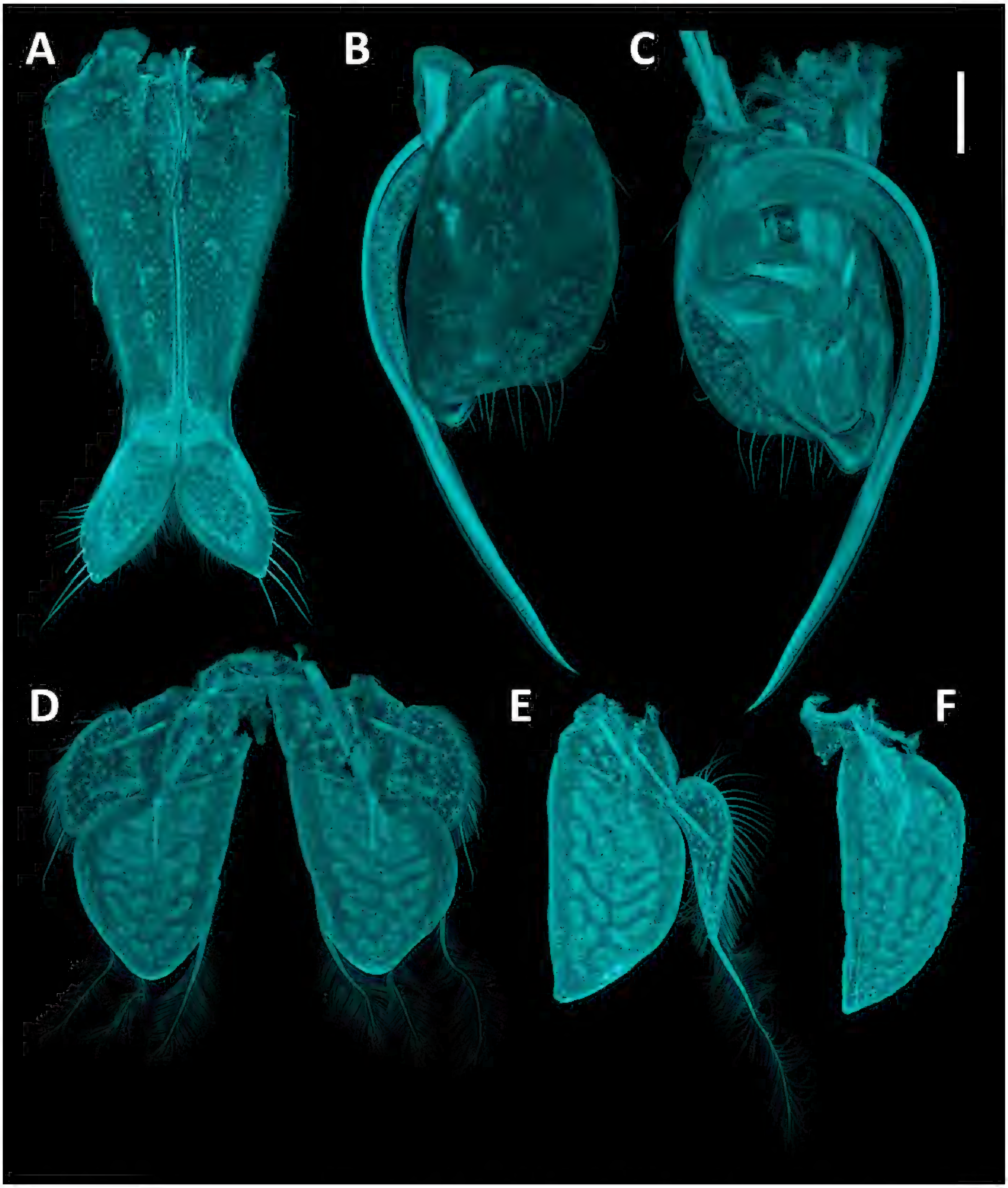

Figure 25. *Haploniscus nyx* sp. nov. male holotype, SKB Hap34. **A.** Pleopod I; **B.** Pleopod II, ventral view; **C.** Pleopod II, dorsal view; **D.** Pleopods III; **E.** Pleopod IV; **F.** Pleopod V. Scale bar: 0.25 mm.

Antenna II (Fig. 23A) length 0.61 body length; article 3 dorsal projection triangular, projection length 0.36 article 3 length; article 5 projection length 0.23 article 5 length; flagellum with 15 articles.

Mandible (Fig. 24B, C) incisor with 5 cusps, left Md *lacinia mobilis* with 4 cusps.

Maxillipeds (Fig. 24A) with 3 coupling hooks each.

Pereopod I (Fig. 23C) length 0.37 body length. **PII** (Fig. 23D) length 0.45 body length. **PIII** (Fig. 23E) length 0.52 body length. **PV** length 0.65 body length. **PVI** length 0.70 body length; P lengths gradually increasing from PI to PVI, PVII shorter than PVI.

Pleopod I (Figs 25A, 26L) medial lobes convexly rounded, tapering to an obtuse point; adjoining at the apex.

Pleopod II (Fig. 25B, C) protopod semi-circular, with distal lobe extending beyond protopod distal margin; endopod stylet 2.1 protopod length.

Female. Differs from male in the following characters:

Body (Fig. 22A) length 2.1 width; oval; anterior body length (Ceph–Prn 4) 0.98 posterior body length (Prn 5–Plt).

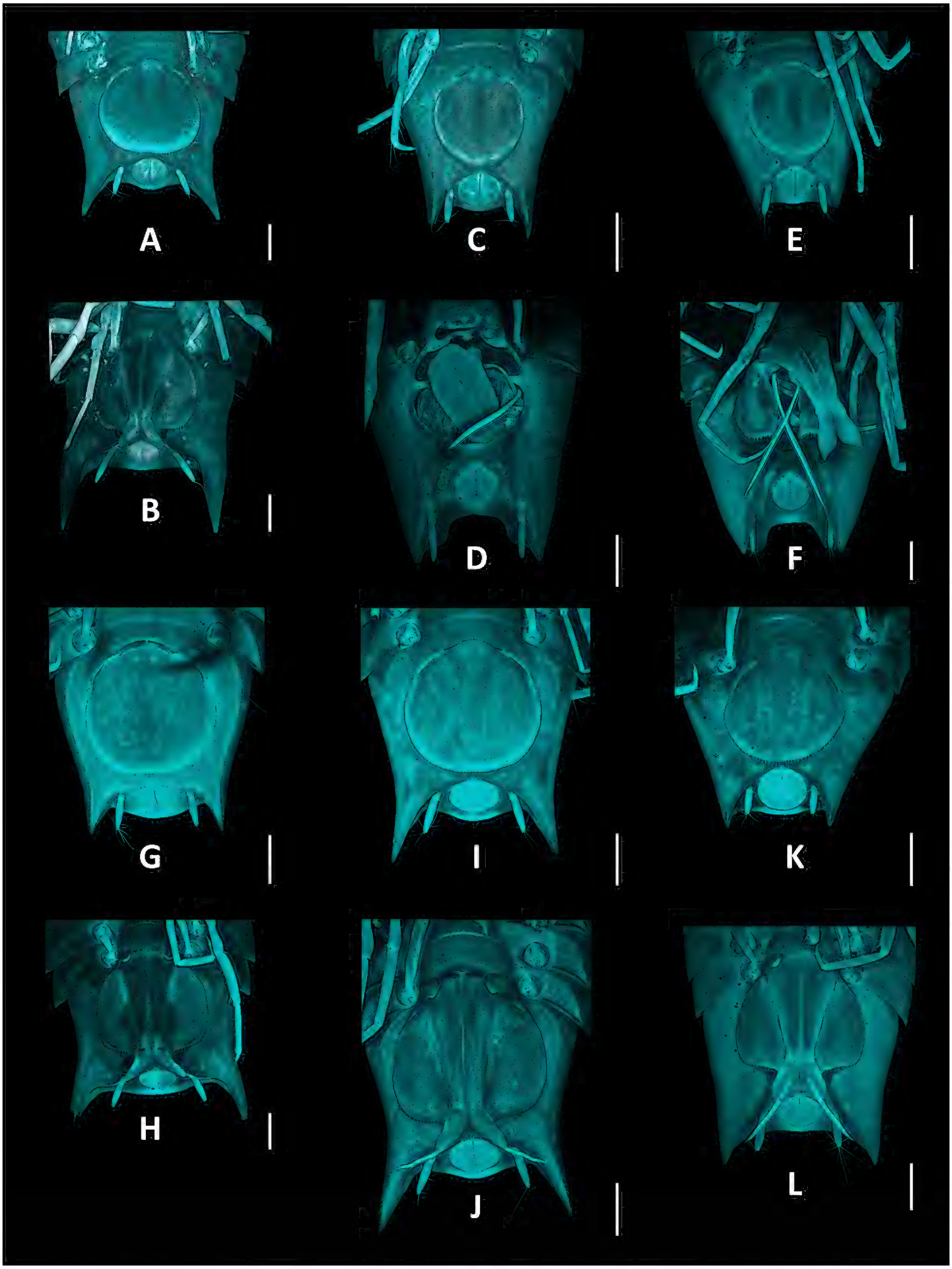

Figure 26. Comparison of pleotelson shapes amongst adult male and female members of the *Haploniscus belyaevi* species complex (CLSM). *H. erebus* sp. nov. female (**A**) and male (**B**) from Knauber et al. (2022); *H. kerberos* sp. nov. female (**C**) and male (**D**); *H. hades* sp. nov. female (**E**) and male (**F**); *H. belyaevi* female (**G**) and male (**H**); *H. apaticus* sp. nov. female (**I**) and male (**J**); *H. nyx* sp. nov. female (**K**) and male (**L**). Scale bars: 0.5 mm.

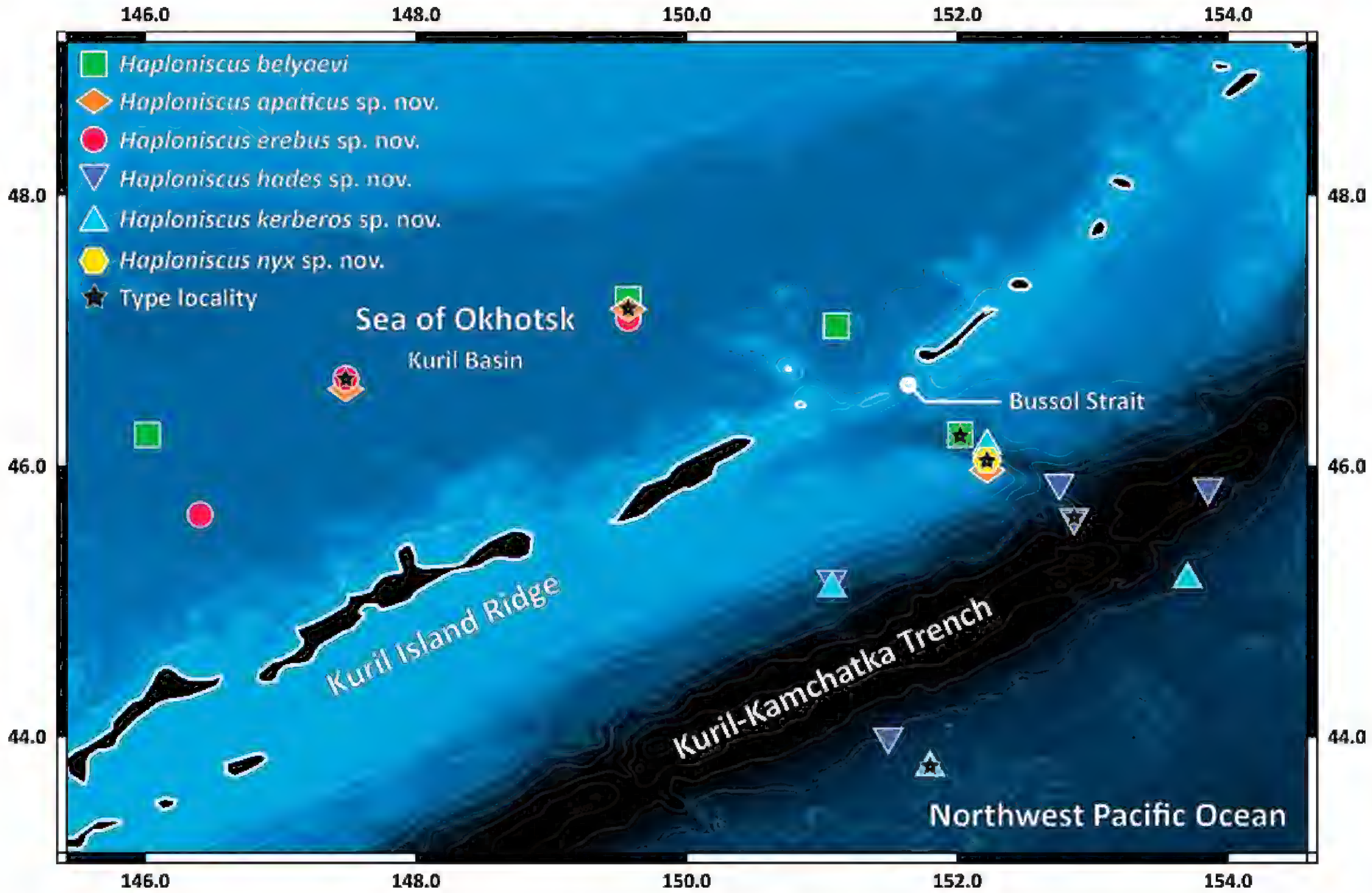

Figure 27. Distribution of haploniscid species of the *belyaevi*-complex in the greater Kuril-Kamchatka Trench and Sea of Okhotsk area of the Northwest Pacific. Stars indicate each species type locality.

Cephalothorax (Fig. 22A, C) length 0.46 width, 0.12 body length, width 0.55 body width; frontal margin width 0.46 Ceph width.

Pereonite 4 (Fig. 22A) lateral margin length 1.05 Prn 5 lateral margin length.

Pleotelson (Figs 22A, 26K) length 0.83 width, 0.27 body length, posterior margin rounded, convex; postero-lateral processes short, 0.19 Plt length.

Antenna I (Fig. 22A) length 0.16 body length; flagellum with 4 articles.

Antenna II (Fig. 22A) length 0.50 body length; flagellum with 15 articles.

Operculum (Fig. 26K) length 0.98 width, 0.66 Plt length; distal margin with numerous, evenly distributed long setae; lateral margins with fewer, evenly distributed short setae.

Identification key to the species of the *Haploniscus belyaevi* species complex based on adult male stages

1 Anterolateral angle of Prn 5 not projecting; Plt posterior margin with tergal plates projecting above uropods, covering them almost completely from dorsal view; Plt with posterolateral tergal ridge terminating on posterolateral process; Plp II elongated, suboval, without distal lobe extending beyond protopod distal margin 2

– Anterolateral angle of Prn 5 with minute acute projection; Plt posterior margin without projecting tergal plates, uropods clearly visible from dorsal view; Plt with posterolateral tergal ridge terminating between uropod insertion and posterolateral process; Plp II semi-circular, with distal lobe extending beyond protopod distal margin 3

2 (1) Rostrum basally with pronounced dorsal bulge; AII article 3 dorsal projection hook-shaped...... *Haploniscus hades* sp. nov.

– Rostrum basally without dorsal bulge; AII article 3 dorsal projection triangular .... *Haploniscus kerberos* sp. nov.

3 (1) Rostrum straight .... *Haploniscus erebus* sp. nov.

– Rostrum curved upwards 4

4 (3) Rostrum anteriorly flat; Prn 1 anterolateral angle with minute, acute projection; Prn 1 anterior margin delicately serrated, setose; Plt rectangular, posterolateral processes curved............ *Haploniscus belyaevi* Birstein, 1963

– Rostrum anteriorly not flat; Prn 1 anterolateral angle not projecting; Plt trapezoidal, posterolateral processes straight...... 5

5 (4) Lateral margin of Prn 4 longer than of Prn 5; Plt posterior margin convex, posterolateral processes oriented posterolaterally; PV–VII lengths distinctly exceeding PI–IV lengths; Plp I medial lobes subtriangular, projecting caudolaterally .... *Haploniscus apaticus* sp. nov.

– Prn 4 and Prn 5 lateral margins of equal length; Plt posterior margin concave, posterolateral processes oriented posteriorly; P lengths gradually increasing from PI to PVI; Plp I medial lobes convexly rounded, tapering to an obtuse point .... *Haploniscus nyx* sp. nov.

Geometric morphometrics

The canonical variate analysis of the pleotelson shapes of *H. kerberos* sp. nov., *H. hades* sp. nov., and *H. belyaevi* revealed the distinction of six groups defined by the species and sex of the analyzed specimens (Fig. 28). A Procrustes ANOVA confirmed that the conducted pleotelson shape analysis was highly significant ($p < 0.01\%$). The male pleotelson shapes of *H. kerberos* sp. nov. and *H. hades* sp. nov. are quite similar, yet distinct, as indicated by their close positioning next to one another, while *H. belyaevi* is far off. The latter species also exhibits the strongest differentiation between male and female pleotelson shapes of any of the three analyzed species. The female pleotelson shape of *H. belyaevi* is much more similar to the ones of the other female specimens of *H. kerberos* sp. nov. and *H. hades* sp. nov. than to its respective males. For *H. kerberos* sp. nov. and *H. hades* sp. nov., male and female specimens are also located much closer to one another.

Genomics

The resulting nuclear genome assemblies are very fragmented, which is expected given their respective low coverage. Statistics of the final assemblies after filtering are shown in Table 4.

All assembled mitochondrial genomes contain the expected 13 protein-coding genes and two rRNAs. The gene order is conserved among the assembled mitochondrial genomes and references, with the sole exception of KBII Hap154, belonging to *Haploniscus hydroniscoides*, having ND6 and 16S rRNA switched (Fig. 29A; not observed in all references) as well as 12S rRNA before ND1 (Fig. 29B; only observed in the reference of *Ichthyoxenos japonensis*).

Levels of intraspecific divergence within the *belyaevi*-complex ranged between 5.5 and 20.5% (Table 5). In comparison, *H. hydroniscoides* scored higher *p*-distances in relation to the *belyaevi*-complex, ranging between 36.1 and 36.7%. Interspecific divergence to the two outgroup species of *Notopais* amounted to 51.7–52%.

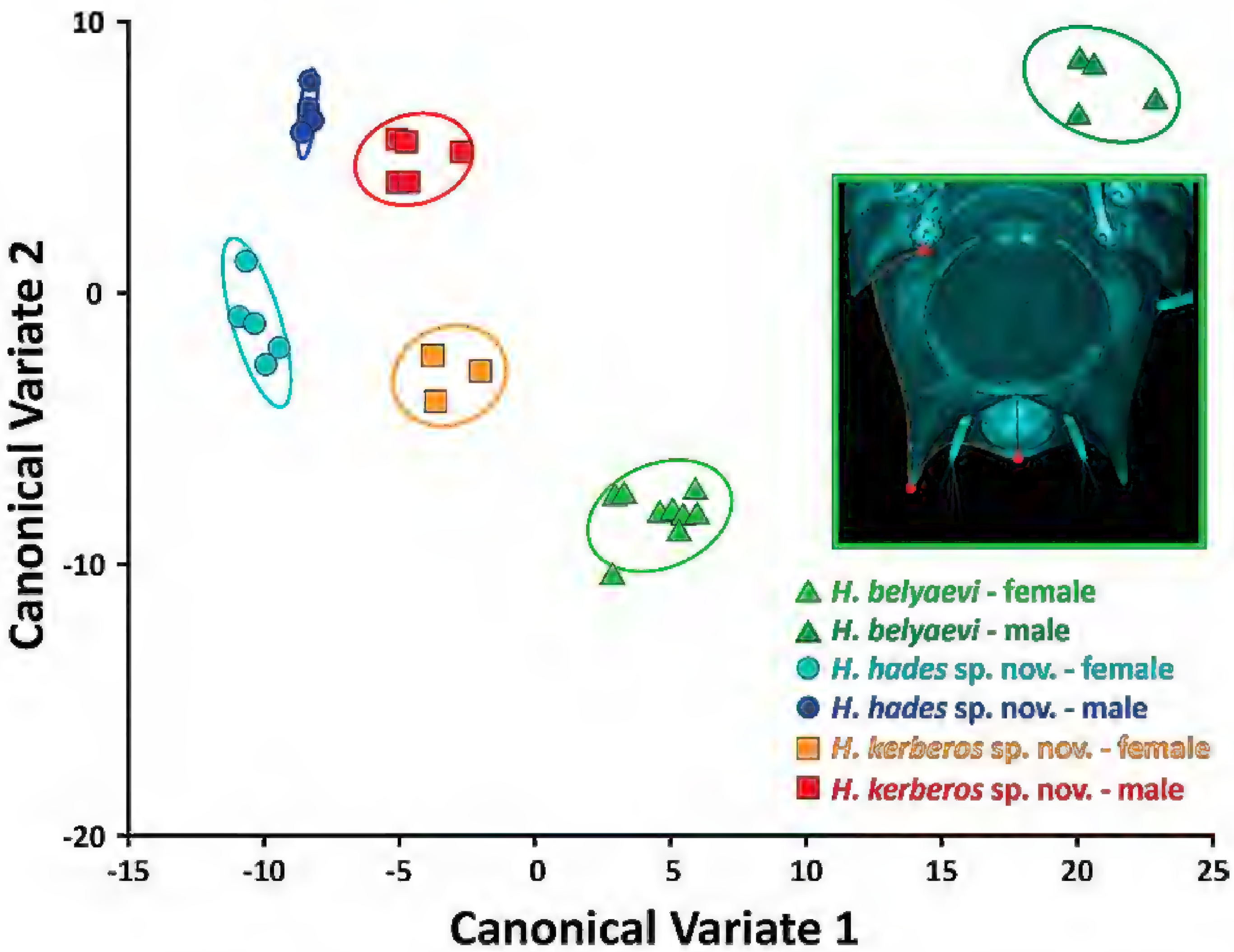

Figure 28. Scatter plot displaying the geometric morphometric analyses of the pleotelson shape from *H. belyaevi*, H. *kerberos* sp. nov., and *H. hades* sp. nov. for both sexes. The underlying data for this analysis stem from landmarking the pleotelson outline from a ventral view using CLSM images and photographs, as illustrated on the right

Table 4. Statistics of the *de novo* assemblies after filtering.

Sample	KBII Hap104	KBII Hap122	KBII Hap154	SKB Hap04	SKB Hap48	SKB Hap49
Species	*H. hades* sp. nov.	*H. kerberos* sp. nov.	*H. hydroniscoides*	*H. belyaevi*	*H. apaticus* sp. nov.	*H. erebus* sp. nov.
Assembler	Spades	Spades	Spades	Platanus	Spades	Platanus
#contigs	647436	610536	568443	26068249	698293	26259349
Total length	877079199	916542958	776628239	1667875350	699113445	2126489036
N50	3054	3254	3931	875	2107	1036
GC (%)	32.46	32.52	33.24	32.14	31.93	32.16
BUSCO arthropoda_odb10 (N = 1013)	C:24.5% [S:24.0%, D:0.5%], F:38.9%, M:36.6%	C:24.2% [S:23.5%, D:0.7%], F:42.3%, M:33.5%	C:28.4% [S:26.5%, D:1.9%], F:38.0%, M:33.6%	C:9.1% [S:9.0%, D:0.1%], F:34.0%, M:56.9%	C:19.6% [S:19.3%, D:0.3%], F:39.2%, M:41.2%	C:12.0% [S:12.0%, D:0.0%], F:37.3%, M:50.7%

Figure 29. Overview of the mitochondrial genome alignment. The alignments were created from assembled sequences and available references in the regions of ND6 and 16S rRNA (**A**) as well as ND1 and 12S rRNA (**B**). Hap04 = *H. belyaevi*; Hap48 = *H. apaticus* sp. nov.; Hap49 = *H. erebus* sp. nov.; Hap104 = *H. hades* sp. nov.; Hap122 = *H. kerberos* sp. nov.; Hap154 = *H. hydroniscoides*.

Table 5. Interspecific divergence within the *belyaevi*-complex and outgroup species. Uncorrected *p*-distances between mitogenomes of the analyzed *belyaevi*-complex members, *H. hydroniscoides* and two outgroup species of the munnopsid genus *Notopais*.

Taxon	*H. hades* sp. nov.	*H. kerberos* sp. nov.	*H. belyaevi*	*H. apaticus* sp. nov.	*H. erebus* sp. nov.	*H. hydroniscoides*	*Notopais* sp. c
H. kerberos sp. nov.	0.066						
H. belyaevi	0.205	0.198					
H. apaticus sp. nov.	0.204	0.199	0.055				
H. erebus sp. nov.	0.203	0.197	0.154	0.156			
H. hydroniscoides	0.363	0.361	0.367	0.364	0.361		
Notopais sp. c	0.598	0.595	0.597	0.598	0.593	0.567	
Notopais sp. p	0.517	0.517	0.518	0.52	0.52	0.497	0.489

Discussion

The present study builds upon the efforts of Knauber et al. (2022), which laid the groundwork for delimitating the closely related species of the *Haploniscus belyaevi* species complex using integrative taxonomy. The close relationships and corresponding overlapping morphological variation of these species made it necessary to reach beyond traditional taxonomic concepts for the Haploniscidae to successfully delineate the members of the *belyaevi*-complex. Our findings demonstrate that the novel species described herein can be told apart more or less clearly based on morphology and molecular data.

Morphological and molecular variation within the belyaevi-complex

The application of reciprocal illumination (Hennig 1965; Lienau et al. 2006) in the *belyaevi*-complex revealed that the primary morphological distinguishing features comprise the shapes of the antennae, the cephalothorax (particularly the rostrum), and the pleotelson (specifically the posterolateral processes). Conversely, other anatomical features, such as the pleopods III–V or the mouthparts, have historically been described in greater detail, yet reportedly exhibit comparatively small variation in the herein described species and the Haploniscidae as a whole (Park 2000; Leese and Brenke 2005; e.g., Brökeland 2010a). While these appendages are illustrated herein to allow for future investigations, their description was shortened as currently their diagnostic value remains low. Instead, the species descriptions were complemented with molecular data using barcode-based molecular diagnoses and mitogenomic data. Levels of interspecific divergence between members of the *belyaevi*-complex using mitogenomic data were of similar magnitude as the ones using COI barcode data (compare Knauber et al. 2022) with slight deviations. The most notable difference between interspecific divergence levels based on mitogenomic and COI barcode data is found between the *belyaevi*-complex and *H. hydroniscoides*, which served as an outgroup in the study from 2022 and herein: interspecific divergence was over 10% higher between those two groups in the mitogenomic data than in the COI data.

Implications for the taxonomy of the Haploniscidae

The phenotypic plasticity of the *belyaevi*-complex is in line with the observation of ontogenetic changes and sexual dimorphism observed in various other studies on haploniscid taxonomy (Brökeland and Raupach 2008; Brökeland 2010b; Brix et al. 2011; Knauber et al. 2022). It underscores the importance of integrative approaches, including the combined consideration of morphological and molecular data as well as novel analysis techniques. As species complexes are relatively common among the Haploniscidae (Brökeland and Raupach 2008; Brökeland 2010a; Knauber et al. 2022), such methodologically broad attempts to uncover their diversity seem essential.

The Haploniscidae, especially the genus *Haploniscus*, reportedly require substantial taxonomic revision (Lincoln 1985; Brökeland 2010a). Historically, taxonomic work on this group has relied on very detailed and extensive descriptions of morphological characters, many of which as of now seem to have low or no diagnostic and species delimitating value. Following these standards to describe everything in great detail renders the description of novel species into a time-consuming endeavor. This issue is further exacerbated by a large number of haploniscid species still awaiting description (unpublished data). In order to resolve the haploniscid taxonomy and complement the species catalogue of this family, future studies should, therefore, carefully evaluate the information content and diagnostic power of the wide range of available data to effectively achieve these aims.

Complementing the belyaevi-complex

Preliminary data from recent sampling campaigns in the North Pacific Aleutian and Japan Trenches in the course of the AleutBio (Brandt 2022) and Hakuho Maru campaigns (Brandt et al. 2024) indicate that the *belyaevi*-complex also occurs there (Knauber, unpublished data). Haploniscid specimens bearing the distinct distal spine on article 5 of the second antenna have been recovered from both of these trenches. Their specific taxonomic affiliation, whether they pertain to the species treated here or represent novel members of the *belyaevi*-complex, remains unclear so far.

Similarly, Gamó (1989) illustrated an immature specimen from the Okinawa Trough, also possessing the characteristic spine on the second antenna. Due to the ontogenetic variability of haploniscid isopods, a species assignment of this juvenile specimen based solely on these illustrations is impossible. Unfortunately, scrutinizing this specimen further is unfeasible as it has been destroyed during analysis. Regardless, this record shows the biogeographic range of the *belyaevi*-complex extends way beyond the greater KKT area.

Outlook

The species composition and biogeographic distribution of the *belyaevi*-complex will be complemented based on novel specimens in the foreseeable future. Given the *belyaevi*-complex's prevalence in the NWP, its composition and distinct distribution (Knauber et al. 2022) raise questions about how these closely related species dispersed and differentiated. Studying the *belyaevi*-complex in an integrative context on a larger scale might thus provide valuable insights into the processes and underlying factors shaping benthic faunal differentiation and distribution patterns in the deep NWP.

Conclusion

The species of the Haploniscidae described herein belong to a complex of closely related species – the first of its kind reported for this isopod family from the Northwest Pacific Ocean. While morphologically diagnostic characters are mostly limited to the relatively distinct adult males, these species exhibit varying biogeographical ranges tied to large-scale bathymetric features. New means of morphological and molecular methods, including the first mitogenomic data for haploniscid isopods, aided in their delineation and might be beneficial for future taxonomic studies on the to-be-revised Haploniscidae and the study of species differentiation in the abysso-hadal Northwest Pacific.

Data availability statement

The associated (meta-)data to these haploniscid records, made available by Knauber et al. (2022) in the Barcode of Life Data System (BoLD System; Ratnasingham and Hebert 2007) available at dx.doi.org/10.5883/DS-NWPHA22, GenBank (Benson et al. 2012) accession numbers OM782497 to OM782662, National Center for Biotechnology Information (NCBI, (Sayers et al. 2022) available at BioProject PRJNA1100257, Ocean Biogeographic Information System (OBIS; Grassle 2000) available at https://ipt.iobis.org/obis-deepsea/resource?r=deep-sea_haploniscid_isopods and Zenodo (European Organization For Nuclear Research, OpenAIRE 2013) available at http://doi.org/10.5281/zenodo.6553796, will be updated accordingly.

Acknowledgements

We thank the crews of the RVs *Sonne* and *Akademik M.A. Lavrentyev* for their work and help in collecting the samples analyzed within this study as well as all scientists, student helpers, and technicians who sorted and managed the collected samples during the international KuramBio II and SokhoBio projects. Special thanks to Anchita Casaubon for her help with geometric morphometrics. The authors also want to thank Damian Baranski and Carola Greve for their help regarding the sequencing lab work. This is contribution #27 of the Senckenberg Ocean Species Alliance (SOSA).

The SokhoBio expedition was organized with financial support from the Russian Science Foundation (Project No. 14-50-00034). Material sorting was funded by the BMBF (German Ministry of Education and Research) grant 03G0857A to Angelika Brandt, University of Hamburg, now Senckenberg Museum, Frankfurt, Germany. Funding for the KuramBio II expedition was provided by the PTJ (Projektträger Jülich) BMBF grant 03G0250A to Angelika Brandt. Further support for these projects was provided by the Russian Foundation for Basic Research (projects 13-04-02144, 16-04-01431), the Council of the President of the Russian Federation (project MK-2599.2013.4), Russian Federation Government grant No 11. G34.31.0010, and a grant of the Presidium of the Far East Branch of RAS (12–I–P30–07). Sequencing was financed through the Holotype Sequencing Project of the LOEWE Centre for Translational Biodiversity Genomics (TBG; grant number LOE WE/1/10/519/03/03.001(0014)/52 of the Hessen State Ministry of Higher Education, Research and the Arts (HMWK)).

References

Agassiz A (1880) Report of the dredging cruise of the U.S. steamer Blake, Commander Bartlett, during the summer of 1880. Science 1: 314–314. https://doi.org/10.1126/science.os-1.27.314-a

Appeltans W, Ahyong ST, Anderson G, Angel MV, Artois T, Bailly N, Bamber R, Barber A, Bartsch I, Berta A, Błażewicz-Paszkowycz M, Bock P, Boxshall G, Boyko CB, Brandão SN, Bray RA, Bruce NL, Cairns SD, Chan T-Y, Cheng L, Collins AG, Cribb T, Curini-Galletti M, Dahdouh-Guebas F, Davie PJF, Dawson MN, De Clerck O, Decock W, De Grave S, de Voogd NJ, Domning DP, Emig CC, Erséus C, Eschmeyer W, Fauchald K, Fautin DG, Feist SW, Fransen CHJM, Furuya H, Garcia-Alvarez O, Gerken S, Gibson D, Gittenberger A, Gofas S, Gómez-Daglio L, Gordon DP, Guiry MD, Hernandez F, Hoeksema BW, Hopcroft RR, Jaume D, Kirk P, Koedam N, Koenemann S, Kolb JB, Kristensen RM, Kroh A, Lambert G, Lazarus DB, Lemaitre R, Longshaw M, Lowry J, Macpherson E, Madin LP, Mah C, Mapstone G, McLaughlin PA, Mees J, Meland K, Messing CG, Mills CE, Molodtsova TN, Mooi R, Neuhaus B, Ng PKL, Nielsen C, Norenburg J, Opresko DM, Osawa M, Paulay G, Perrin W, Pilger JF, Poore GCB, Pugh P, Read GB, Reimer JD, Rius M, Rocha RM, Saiz-Salinas JI, Scarabino V, Schierwater B, Schmidt-Rhaesa A, Schnabel KE, Schotte M, Schuchert P, Schwabe E, Segers H, Self-Sullivan C, Shenkar N, Siegel V, Sterrer W, Stöhr S, Swalla B, Tasker ML, Thuesen EV, Timm T, Todaro MA, Turon X, Tyler S, Uetz P, van der Land J, Vanhoorne B, van Ofwegen LP, van Soest RWM, Vanaverbeke J, Walker-Smith G, Walter TC, Warren A, Williams GC, Wilson SP, Costello MJ (2012) The Magnitude of Global Marine Species Diversity. Current Biology 22: 2189–2202. https://doi.org/10.1016/j.cub.2012.09.036

Benson DA, Cavanaugh M, Clark K, Karsch-Mizrachi I, Lipman DJ, Ostell J, Sayers EW (2012) GenBank. Nucleic Acids Research 41: D36–D42. https://doi.org/10.1093/nar/gks1195

Birstein JA (1963) Deep water isopods (Crustacea, Isopoda) of the north-western part of the Pacific Ocean. Nauka Publishing House, USSR Academy of Sciences, P.P. Shirshov Institute of Oceanography, Moscow, 317 pp.

Birstein JA (1971) Additions to the fauna of isopods (Crustacea: Isopoda) of the Kuril-Kamchatka Trench. Part 2. Asellota-2. Trudy Instituta Okeanologii Akademiya Nauk SSR, 162–238.

Bolger AM, Lohse M, Usadel B (2014) Trimmomatic: a flexible trimmer for Illumina sequence data. Bioinformatics 30: 2114–2120. https://doi.org/10.1093/bioinformatics/btu170

Boyko CB, Bruce NL, Hadfield KA, Merrin KL, Ota Y, Poore GCB, Taiti S, Schotte M, Wilson GDF (2023) World Register of Marine Species - Database: Haploniscidae Hansen, 1916. World register of marine species. http://www.marinespecies.org/aphia.php?p=taxdetails&id=118254#sources [March 7, 2018]

Brandt A (2016) Kuril Kamchatka Biodiversity Studies II - RV Sonne SO250, Tomakomai-Yokohama (Japan), 16.08.-26.09.2016. University of Hamburg, Hamburg, Germany. Cruise report, 174 pp.

Brandt A (2022) SO293 AleutBio (Aleutian Trench Biodiversity Studies) Cruise Report. Cruise report, 209 pp. https://doi.org/10.48433/cr_so293

Brandt A, Malyutina M (2013) The German-Russian deep-sea expedition KuramBio (Kurile Kamchatka Biodiversity Studies) to the Kuril-Kamchatka Trench and abyssal plain on board of the R/V Sonne. Vladivostok, Russia. Cruise report, 100 pp. http://oceanrep.geomar.de/36686/ [March 28, 2018]

Brandt A, Elsner N, Brenke N, Golovan O, Malyutina MV, Riehl T, Schwabe E, Würzberg L (2013) Epifauna of the Sea of Japan collected via a new epibenthic sledge equipped with camera and environmental sensor systems. Deep Sea Research Part II: Topical Studies in Oceanography 86–87: 43–55. https://doi.org/10.1016/j.dsr2.2012.07.039

Brandt A, Brix S, Riehl T, Malyutina M (2020) Biodiversity and biogeography of the abyssal and hadal Kuril-Kamchatka trench and adjacent NW Pacific deep-sea regions. PrOce 181: 102232. https://doi.org/10.1016/j.pocean.2019.102232

Brandt A, Bergmeier F, Casaubon A, Kano Y, Kelch A, Knauber H, Okamoto K, Ohta M, Shiraki S, Yamamoto D, Kojima S (2024) Benthos meets plankton: Isopods sampled in the Japan Trench by means of plankton nets fixed to large bottom trawls. Marine Biodiversity. https://doi.org/10.21203/rs.3.rs-3801343/v1

Brenke N (2005) An epibenthic sledge for operations on marine soft bottom and bedrock. Marine Technology Society Journal 39: 10–21. https://doi.org/10.4031/002533205787444015

Brix S, Riehl T, Leese F (2011) First genetic data for species of the genus *Haploniscus* Richardson, 1908 (Isopoda: Asellota: Haploniscidae) from neighbouring deep-sea basins in the South Atlantic. Zootaxa 2838: 79–84. https://doi.org/10.11646/zootaxa.2838.1.5

Brökeland W (2010a) Description of four new species from the *Haploniscus unicornis* Menzies, 1956 complex (Isopoda: Asellota: Haploniscidae). Zootaxa 2536: 1–35. https://doi.org/10.11646/zootaxa.2536.1.1

Brökeland W (2010b) Redescription of *Haploniscus rostratus* (Menzies, 1962) (Crustacea: Peracarida: Isopoda) with observations on the postmarsupial development, size ranges and distribution. Zootaxa 2521: 1–25. https://doi.org/10.11646/zootaxa.2521.1.1

Brökeland W, Raupach MJ (2008) A species complex within the isopod genus *Haploniscus* (Crustacea: Malacostraca: Peracarida) from the Southern Ocean deep sea: a morphological and molecular approach. Zoological Journal of the Linnean Society 152: 655–706. https://doi.org/10.1111/j.1096-3642.2008.00362.x

Brökeland W, Svavarsson J (2017) Distribution of haploniscids (Isopoda, Asellota, Haploniscidae) in Icelandic waters, with description of *Haploniscus astraphes* n. sp. from the Iceland basin and the Southeast Atlantic Ocean. Zootaxa 4231: 301–326. https://doi.org/10.11646/zootaxa.4231.3.1

Casaubon A, Riehl T (2024) Shape matters: investigating the utility of geometric morphometric techniques in the deep-sea isopod family Macrostylidae (Isopoda: Asellota). Frontiers in Marine Science 11. https://doi.org/10.3389/fmars.2024.1380594

Coleman CO (2003) “Digital inking”: How to make perfect line drawings on computers. Organisms, Diversity and Evolution 3: 303–304. https://doi.org/10.1078/1439-6092-00081

Dallwitz MJ (1980) A general system for coding taxonomic descriptions. Taxon, 41–46. https://doi.org/10.2307/1219595

Dallwitz MJ, Paine TA, Zurcher EJ (1999) User’s guide to the DELTA Editor.

Dierckxsens N, Mardulyn P, Smits G (2017) NOVOPlasty: de novo assembly of organelle genomes from whole genome data. Nucleic acids research 45: e18–e18. https://doi.org/10.1093/nar/gkw955

Donath A, Jühling F, Al-Arab M, Bernhart SH, Reinhardt F, Stadler PF, Middendorf M, Bernt M (2019) Improved annotation of protein-coding genes boundaries in metazoan mitochondrial genomes. Nucleic Acids Research 47: 10543–10552. https://doi.org/10.1093/nar/gkz833

Dreutter S, Steffen M, Arbizu PM, Brandt A (2020) Will the “top five” deepest trenches lose one of their members? Progress in Oceanography 181: 102258. https://doi.org/10.1016/j.pocean.2019.102258

European Organization For Nuclear Research, OpenAIRE (2013) Zenodo. https://doi.org/10.25495/7GXK-RD71

Gamó S (1989) Some bathyal cumacean and isopod crustaceans from the Okinawa Trough, the East China Sea, with descriptions of a new genus and five new species. Bulletin of the Biogeographical Society of Japan 44: 20.

Goffredi S, Hurtado L, Hallam S, Vrijenhoek R (2003) Evolutionary relationships of deep-sea vent and cold seep clams (Mollusca: Vesicomyidae) of the “*pacifica/lepta*” species complex. Marine Biology 142: 311–320. https://doi.org/10.1007/s00227-002-0941-3

Golovan OA, Błażewicz M, Brandt A, Jażdżewska AM, Jóźwiak P, Lavrenteva AV, Malyutina MV, Petryashov VV, Riehl T, Sattarova VV (2019) Diversity and distribution of peracarid crustaceans (Malacostraca) from the abyss adjacent to the Kuril-Kamchatka Trench. Marine Biodiversity 49: 1343–1360. https://doi.org/10.1007/s12526-018-0908-3

GRASS Development Team (2020) Geographic Resources Analysis Support System (GRASS) Software. Open Source Geospatial Foundation. http://grass.osgeo.org [August 31, 2020]

Grassle JF (2000) The Ocean Biogeographic Information System (OBIS): an online, worldwide atlas for accessing, modeling and mapping marine biological data in a multidimensional geographic context. Oceanography 13: 5–7. https://doi.org/10.5670/oceanog.2000.01

Gurevich A, Saveliev V, Vyahhi N, Tesler G (2013) QUAST: quality assessment tool for genome assemblies. Bioinformatics 29: 1072–1075. https://doi.org/10.1093/bioinformatics/btt086

Hansen HJ (1916) Crustacea Malacostraca, III. V. The order Isopoda. In: The Danish Ingolf-Expedition. Copenhagen, 1–262.

Hennig W (1965) Phylogenetic systematics. Annual review of entomology 10: 97–116. https://doi.org/10.1146/annurev.en.10.010165.000525

Hessler RR (1970) 15 The Desmosomatidae (Isopoda, Asellota) of the Gay Head-Bermuda transect. University of California Press, 185 pp. https://escholarship.org/uc/item/1mn198vx [March 27, 2020]

Hessler RR, Jumars PA (1974) Abyssal community analysis from replicate box cores in the central North Pacific. Deep Sea Research and Oceanographic Abstracts 21: 185–209. https://doi.org/10.1016/0011-7471(74)90058-8

Hütter T, Ganser MH, Kocher M, Halkic M, Agatha S, Augsten N (2020) DeSignate: detecting signature characters in gene sequence alignments for taxon diagnoses. BMC Bioinformatics 21: 151. https://doi.org/10.1186/s12859-020-3498-6

Johannsen N, Lins L, Riehl T, Brandt A (2020) Changes in species composition of Haploniscidae (Crustacea: Isopoda) across potential barriers to dispersal in the Northwest Pacific. Progress in Oceanography: 180. https://doi.org/10.1016/j.pocean.2019.102233

Kajitani R, Toshimoto K, Noguchi H, Toyoda A, Ogura Y, Okuno M, Yabana M, Harada M, Nagayasu E, Maruyama H (2014) Efficient de novo assembly of highly heterozygous genomes from whole-genome shotgun short reads. Genome research 24: 1384–1395. https://doi.org/10.1101/gr.170720.113

Klingenberg CP (2011) MorphoJ: an integrated software package for geometric morphometrics. Molecular Ecology Resources 11: 353–357. https://doi.org/10.1111/j.1755-0998.2010.02924.x

Knauber H, Silberberg JR, Brandt A, Riehl T (2022) Evolution and biogeography of the *Haploniscus belyaevi* species complex (Isopoda: Haploniscidae) revealed by means of integrative taxonomy. Systematics and Biodiversity 20: 1. https://doi.org/10.1080/14772000.2022.2099477

Knowlton N (1993) Sibling species in the sea. Annual review of ecology and systematics 24: 189–216. https://doi.org/10.1146/annurev.es.24.110193.001201

Leese F, Brenke N (2005) *Chauliodoniscus coronatus* sp. nov., a new deep-sea species from the Angola Basin (Crustacea, Isopoda, Asellota, Janiroidea, Haploniscidae). Organisms Diversity & Evolution 5: 189–201. https://doi.org/10.1016/j.ode.2004.11.003

Lienau EK, DeSalle R, Rosenfeld JA, Planet PJ (2006) Reciprocal Illumination in the Gene Content Tree of Life. Systematic Biology 55: 441–453. https://doi.org/10.1080/10635150600697416

Lincoln RJ (1985) The marine fauna of New Zealand deep-sea Isopoda Asellota family Haploniscidae. New Zealand Oceanographic Institute Memoir Vol. 94, 55 pp.

Malyutina MV, Brandt A, Ivin VI (2015) The Russian-German deep-sea expedition SokhoBio (Sea of Okhotsk Biodiversity Studies) to the Kurile Basin of the Sea of Okhotsk on board of the R/V Akademik M. A. Lavrentyev. Vladivostok, Russia. Cruise report, 102 pp.

Malyutina MV, Chernyshev AV, Brandt A (2018) Introduction to the SokhoBio (Sea of Okhotsk Biodiversity Studies) expedition 2015. Deep Sea Research Part II 154: 1–9. https://doi.org/10.1016/j.dsr2.2018.08.012

Manni M, Berkeley MR, Seppey M, Simão FA, Zdobnov EM (2021) BUSCO update: novel and streamlined workflows along with broader and deeper phylogenetic coverage for scoring of eukaryotic, prokaryotic, and viral genomes. Molecular Biology and Evolution 38: 4647–4654. https://doi.org/10.1093/molbev/msab199

McLaughlin EL, Wilson NG, Rouse GW (2023) Resolving the taxonomy of the Antarctic feather star species complex *Promachocrinus 'kerguelensis'* (Echinodermata: Crinoidea). Invertebrate Systematics 37: 498–527. https://doi.org/10.1071/IS22057

Michels J, Büntzow M (2010) Assessment of Congo red as a fluorescence marker for the exoskeleton of small crustaceans and the cuticle of polychaetes. Journal of Microscopy 238: 95–101. https://doi.org/10.1111/j.1365-2818.2009.03360.x

Monin AS (1983) The Research Vessel "Vityaz" and her Expeditions (1949–1979). Nauka Publishing House, USSR Academy of Sciences, P.P. Shirshov Institute of Oceanography, Moscow, 392 pp.

Mora C, Tittensor DP, Adl S, Simpson AGB, Worm B (2011) How Many Species Are There on Earth and in the Ocean? PLOS Biology 9: e1001127. https://doi.org/10.1371/journal.pbio.1001127

Park J-Y (2000) A revision of the isopod genus Mastigoniscus (Asellota, Haploniscidae) with descriptions of three new species. Zoosystematics and Evolution 76: 195–229. https://doi.org/10.1002/mmnz.20000760204

Prjibelski A, Antipov D, Meleshko D, Lapidus A, Korobeynikov A (2020) Using SPAdes De Novo Assembler. Current Protocols in Bioinformatics 70: e102. https://doi.org/10.1002/cpbi.102

QGIS.org (2020) QGIS Geographic Information System. Open Source Geospatial Foundation Project. http://qgis.org [August 31, 2020]

Ratnasingham S, Hebert PDN (2007) BOLD: The Barcode of Life Data System (www.barcodinglife.org). Molecular Ecology Notes 7: 355–364. https://doi.org/10.1111/j.1471-8286.2007.01678.x

Rex MA, Etter RJ (2010) Deep-sea biodiversity: pattern and scale. Harvard University Press, Boston, MA, 354 pp.

Richardson H (1908) Some new Isopoda of the superfamily Aselloidea from the Atlantic coast of North America. Proceedings of the United States National Museum, 71–86. https://doi.org/10.5479/si.00963801.35-1633.71

Riehl T, Brandt A (2010) Descriptions of two new species in the genus *Macrostylis* Sars, 1864 (Isopoda, Asellota, Macrostylidae) from the Weddell Sea (Southern Ocean), with a synonymisation of the genus *Desmostylis* Brandt, 1992 with *Macrostylis*. ZooKeys 57: 9–49. https://doi.org/10.3897/zookeys.57.310

Riehl T, Wilson GDF, Hessler RR (2012) New Macrostylidae Hansen, 1916 (Crustacea: Isopoda) from the Gay Head-Bermuda transect with special consideration of sexual dimorphism. Zootaxa 3277: 1–26. https://doi.org/10.11646/zootaxa.3277.1.1

Riehl T, Brenke N, Brix S, Driskell A, Kaiser S, Brandt A (2014) Field and laboratory methods for DNA studies on deep-sea Isopod Crustaceans. Polish Polar Research 35: 203–224. https://doi.org/10.2478/popore-2014-0018

Rohlf FJ (2015) The tps series of software. Hystrix 26: 9–12. https://doi.org/10.4404/hystrix-26.1-11264

Sayers EW, Bolton EE, Brister JR, Canese K, Chan J, Comeau DC, Connor R, Funk K, Kelly C, Kim S, Madej T, Marchler-Bauer A, Lanczycki C, Lathrop S, Lu Z, Thibaud-Nissen F, Murphy T, Phan L, Skripchenko Y, Tse T, Wang J, Williams R, Trawick BW, Pruitt KD, Sherry ST (2022) Database resources of the national center for biotechnology information. Nucleic Acids Research 50: D20–D26. https://doi.org/10.1093/nar/gkab1112

Schnurr S, Osborn KJ, Malyutina M, Jennings R, Brix S, Driskell A, Svavarsson J, Arbizu PM (2018) Hidden diversity in two species complexes of munnopsid isopods (Crustacea) at the transition between the northernmost North Atlantic and the Nordic Seas. Marine Biodiversity 48: 813–843. https://doi.org/10.1007/s12526-018-0877-6

SOSA, Brandt A, Chen C, Engel L, Esquete P, Horton T, Jażdżewska A, Johannsen N, Kaiser S, Kihara T, Knauber H, Kniesz K, Landschoff J, Lörz A-N, Machado F, Martínez-Muñoz C, Riehl T, Serpell-Stevens A, Sigwart J, Tandberg AH, Tato R, Tsuda M, Vončina K, Watanabe H, Wenz C, Williams J (2024) Ocean Species Discoveries 1–12 — A primer for accelerating marine invertebrate taxonomy. Biodiversity Data Journal 12: e128431. https://doi.org/10.3897/BDJ.12.e128431

Silva CNS, Murphy NP, Bell JJ, Green BS, Duhamel G, Cockcroft AC, Hernández CE, Strugnell JM (2021) Global drivers of recent diversification in a marine species complex. Molecular Ecology 30: 1223–1236. https://doi.org/10.1111/mec.15780

Tamura K, Stecher G, Kumar S (2021) MEGA11: Molecular Evolutionary Genetics Analysis Version 11. Molecular Biology and Evolution 38: 3022–3027. https://doi.org/10.1093/molbev/msab120

Tillich M, Lehwark P, Pellizzer T, Ulbricht-Jones ES, Fischer A, Bock R, Greiner S (2017) GeSeq–versatile and accurate annotation of organelle genomes. Nucleic Acids Research 45: W6–W11. https://doi.org/10.1093/nar/gkx391

Tyler PA (2002) Deep-sea eukaryote ecology of the semi-isolated basins off Japan. Journal of Oceanography 58: 333–341. https://doi.org/10.1023/A:1015817910449

Vrijenhoek RC (2009) Cryptic species, phenotypic plasticity, and complex life histories: Assessing deep-sea faunal diversity with molecular markers. Deep Sea Research Part II: Topical Studies in Oceanography 56: 1713–1723. https://doi.org/10.1016/j.dsr2.2009.05.016

Wilson GDF (2008) A review of taxonomic concepts in the Nannoniscidae (Isopoda, Asellota), with a key to the genera and a description of *Nannoniscus oblongus* Sars. Zootaxa 1680: 1–24. https://doi.org/10.11646/zootaxa.1680.1.1

Supplementary material 1

Genome Sequencing-Methods

Authors: Tilman Schell
Data type: pdf
Explanation note: Detailed overview about the methods used for genome assembly.
Copyright notice: This dataset is made available under the Open Database License (http://opendatacommons.org/licenses/odbl/1.0/). The Open Database License (ODbL) is a license agreement intended to allow users to freely share, modify, and use this Dataset while maintaining this same freedom for others, provided that the original source and author(s) are credited.
Link: https://doi.org/10.3897/zse.101.137663.suppl1